

People's Democratic Republic of Algeria
Ministry of Higher Education and Scientific Research

University of Amar Telidji - Laghouat



FACULTY OF TECHNOLOGY
MECHANICAL ENGINEERING DEPARTMENT



Graduation thesis

Presented to obtain the diploma of

MASTER

Domain : Science and Technology

Section : Mechanical Engineering

Speciality : Energetics

Theme

*Natural convection of a nanofluid in
C-shaped enclosures*

Candidates:

BENLEHBIB Afif Bouziane

LOKBAICHI Oussama

Board of Examiners

Mr. Ahmed BENCHATTI	Pr.	Univ. Laghouat	Chairperson
Mme. Badia GHERNAOUT	Pr.	Univ. Laghouat	Supervisor
Mme. Maria hannane REGUE	M.C. B	Univ. Laghouat	Examiner

2022/2023

Abstract

In this thesis a numerical study has been carried out on the problem of natural convection and heat transfer using nanofluid (Cu-Water (H₂O)) and (TiO₂-Water (H₂O)) which is the mixture between water and nanoparticles in a c-shaped enclosure. Our problem was defined for a type of geometry (a c-shaped enclosure with different (AR = 0.2,0.4,0.6,0.8) aspect ratio, the flow is generated by heat transfer by free (natural) convection. In our simulation we used four concentrations of nanoparticles, for each concentration the Rayleigh number varied between 10³ and 10⁶. The results obtained for different Rayleigh numbers (Ra =10³, Ra =10⁴, Ra=10⁵, Ra =10⁶) show an increase in average Nusselt due to the increase in volume fraction. For all volume fractions ($\phi =0$, $\phi =0.03$, $\phi =0.06$, $\phi =0.1$), the increase in average Nusselt number is due to the increase in Rayleigh number. Taking into consideration these results the improvement of flow efficiency and heat transfer efficiency is related to the variation of Rayleigh number with volume fraction.

Key words: Natural convection, Nanofluids, Nusselt, Rayleigh, c-shaped enclosure.

Résumé

Dans cet these on a effectué une étude numérique sur le problème de la convection naturelle et le transfert thermique par utilisation de nano-fluide (Cu-Eau (H₂O)) and (TiO₂-Eau (H₂O)) qui est le mélange entre l'eau et des nanoparticules dans une cavité type c. Les calculs ont été effectués par l'utilisation du code de calcul « ANSYS FLUENT » qui utilise la méthode des volumes finis ; Notre problème a été défini pour un type de géométrie (une cavité type c avec different (AR = 0.2,0.4,0.6,0.8) le rapport d'aspect, l'écoulement est généré par le transfert de chaleur par convection libre (naturelle). Dans notre simulation nous avons utilisé quatre concentrations de nano-particules, pour chaque concentration le nombre de Rayleigh dont la variation est entre varié entre 10³ et 10⁶. Les résultats obtenus pour différents nombre de Rayleigh (Ra =10³, Ra =10⁴, Ra=10⁵, Ra =10⁶) montrent une augmentation de Nusselt moyen à cause de l'augmentation de la fraction volumique. Pour toutes les fractions volumiques ($\phi =0$, $\phi =0.03$, $\phi =0.06$, $\phi =0.1$), l'élevation de Nombre de Nusselt moyen à cause de la croissance de nombre de Rayleigh. Tenant en consideration ces resultats l'amélioration de l'efficacité de l'écoulement et le rendement du transfert de chaleur est liée à la variation de nombre de Rayleigh avec la fraction volumique.

Mots clés: Convection naturelle, Nano-fluides, Nusselt, Rayleigh, cavité type c.

المخلص:

في هذا العمل تم إجراء دراسة عديدة حول مشكلة الحمل الحراري الطبيعي ونقل الحرارة باستخدام السوائل النانوية (Cu- Water (H₂O)) و (TiO₂-Water (H₂O)) وهو الخليط بين الماء والجسيمات النانوية في حاوية على شكل حرف C. تم تحديد مشكلتنا لنوع من الهندسة (حاوية على شكل حرف C مع نسبة عرض و ارتفاع مختلفة (AR = 0.2,0.4,0.6,0.8) ، يتم إنشاء التدفق عن طريق نقل الحرارة عن طريق الحمل الحراري الحر (الطبيعي). في المحاكاة التي أجريناها ، استخدمنا أربعة تركيزات من الجسيمات النانوية ، لكل تركيز تراوح رقم Rayleigh بين 10³ و 10⁶. النتائج التي تم الحصول عليها لأرقام Rayleigh المختلفة (Ra = 10³ ، Ra = 10⁴ ، Ra = 10⁵ ، Ra = 10⁶) تظهر زيادة في متوسط Nusselt بسبب الزيادة في الكسر الحجمي. بالنسبة لجميع نسب الحجم ($\phi = 0$ ، $\phi = 0.03$ ، $\phi = 0.06$ ، $\phi = 0.1$) ، ترجع الزيادة في متوسط رقم Nusselt إلى الزيادة في رقم Rayleigh. مع الأخذ في الاعتبار هذه النتائج ، يرتبط تحسين كفاءة التدفق وكفاءة نقل الحرارة باختلاف رقم Rayleigh مع نسب الحجم .

الكلمات المفتاحية: الحمل الحراري الطبيعي ، الموائع النانوية ، Nusselt ، Rayleigh ، حاوية على شكل C.

DEDICATION

we dedicate this humble work :

To our dear Fathers and Mothers.

To our dear Brothers and Sisters.

To our dear and faithful friends.

To the entier Mechanical Engineering class of 2023.

APPRECIATIONS

we would like to take this opportunity to thank our supervisor, Madame Badia GHERNAOUT, for all what she has done for us, advising, helping and assisting us along the way of this final year project.

At the same time, we would like to thank the members of the Jury for their interest in reading and examining this modest work.

we would also like to thank all the teachers in the mechanical engineering department who contributed so much to the success of this work.

Finally, we would like to thank all the people who contributed in any way to the realization of this work.

TABLE OF CONTENTS

DEDICATION

APPRECIATIONS

TABLE OF CONTENTS

Nomenclature

LIST OF FIGURES

General introduction:.....1

CHAPTER I : GENERAL BACKGROUND AND BIBLIOGRAPHICAL STUDY

I-1 General background of heat transfer:.....4

I-1-1 Introduction:.....4

I-1-2 Definitions:.....4

I-2 Heat transfer:.....4

I-2-1 Conductive heat transfer:.....5

I-2-2 Radiant heat transfer:5

I-2-3 Heat transfer by convection :.....6

I-2-3-1 Different types of convection:.....8

a) Forced convection:.....8

b) Natural convection.....9

c) Mixed convection:10

I-3 The Dimensionless Numbers:11

1- Number of Prandtl:11

2- Number of Grashof:.....11

3- Rayleigh number:12

4- Nusselt number:.....12

I-4 Nanofluids.....	13
I-4-1 Definition of nanofluid:.....	13
I-4-2 Types of nanoparticles:.....	14
I-4-3 Applications of nanofluids:.....	14
I-4-4 Advantages of Nano-fluids:	16
I-4-5 Disadvantages of Nano-fluids:	16
I-5 BIBLIOGRAPHICAL STUDY.....	18
I-5-1 Bibliographic summary :.....	18
CHAPTER II : Mathematical modeling	
II-1 Introduction :.....	26
II-2 Mathematical modeling :.....	26
II-3 Thermophysical properties:	28
II-4 Adimensionalization of equations :.....	29
CHAPTER III : Numerical method	
III-1 Introduction :	32
III-2 Calculation procedures:.....	32
III-3 Creation of the geometry:.....	34
III-4 The mesh:.....	37
III-5 Configuration:.....	39
Conclusion:.....	47
CHAPTER IV: Results and discussion	
IV-1 Introduction:.....	48
IV-2 Mesh effect:	48
IV-3 Results validation:	50
IV-4 Presentation of result:	52

4.1 Rayleigh number effect:.....	52
a) For water-cu:	53
b) for Water-TiO ₂ :.....	57
4.2 effect of aspect ratio:	59
a) For water-cu:	60
b) for Water-TiO ₂ :.....	62
4.3 volume fraction effect:.....	64
a) For water-cu:.....	64
b) For Water-TiO ₂ :.....	66
GENERAL CONCLUSION.....	68
Perspectives	69
BIBLIOGRAPHY	70

Nomenclature

AR: aspect ratio of enclosure

C_p: specific heat, J kg⁻¹ K⁻¹

g: gravitational acceleration, m s⁻²

h: heat transfer coefficient, W m⁻² K

H: enclosure height, m

k: thermal conductivity, W m⁻¹ K⁻¹

L: thickness of enclosure, m

Nu: Nusselt number

p: pressure, N m⁻²

P: dimensionless pressure

Pr: Prandtl number

q: heat flux, W m⁻²

Ra: Rayleigh number

T: dimensional temperature, K

u,v: dimensional velocities components in x and y direction, m s⁻¹

U, V: dimensionless velocities components in X and Y direction

x,y: dimensional Cartesian coordinates, m

X, Y: dimensionless Cartesian coordinates

Greek symbols

α: thermal diffusivity, m² s

β: thermal expansion coefficient, K⁻¹

θ: dimensionless temperature

μ: dynamic viscosity, kg m⁻¹ s

η : kinematic viscosity, $m^2 s$

ρ : density, $kg m^{-3}$

ϕ : volume fraction of the nanoparticles

Subscripts

c: cold

f: fluid

h: hot

nf: nanofluid

s: solid particles

w: wall

LIST OF FIGURES

Figure I-1: Principle of heat conduction.....	5
Figure I-2: Principle of radiation heat transfer.....	6
Figure I-3 : Action of moving fluid in convection.....	7
Figure I-4: The phenomenon of forced convection.....	8
Figure I-5: Presentation of convection in a pan.....	9
Figure I-6: Mixed convection, assisted.....	10
Figure 1- 7: Right triangular cavity containing a right triangular heat source under the influence of a magnetic field, study by S.M. Aminossadati.....	21
Figure 1- 8: Natural convection in a square cavity filled with nanofluid; geometrical description of the problem studied by A. Bouhelal et al.....	22
Figure 1- 9: Natural convection in a C-shaped cavity filled with ferrofluid; problem studied by S.Mojumder et al,.....	23
Figure. 1-10: A schematic view of the C-shaped enclosure considered in the present study.....	24
Fig. II-1.: A schematic view of the C-shaped enclosure considered in the present study.....	27
Figure III-1: Software launch window.....	32
Figure III-2: Workbench main menu.....	33
Figure III-3 Creating a fluid fluent (project).....	33
Figure III-4: fluid project project scheme.....	34
Figure III-5. Creating a geometric model (Design Modeler).....	35
Figure III-6. Sketch creation.....	35
Figure III-7. Sketch creation.....	36
Figure III-8. Operation completed.....	36

Figure III-9. Project scheme.....	37
Figure III-10. Mesh.....	37
Figure III-11. Configuration of the simulation on fluent.....	39
Figure III-12. ANSYS FLUENT.....	39
Figure III-13. General CFD parameters.....	40
Figure III-14. Setup of the analysis model.....	41
Figure III-15. Selection of fluid zone.....	41
Figure III-16. Selection of materials.....	42
Figure III-17. Boundary condition.....	43
Figure III-18: Initialization of the solution.....	44
Figure III-19: Choosing the number of iterations.....	44
Figure III-20: Evolution of residuals for a cavity filled with nanofluid (Cu/water), $\phi= 0.01$, $Ra = 10^6$	45
Figure III-21: calculation of temperature and displaying the isotherm line.....	46
Figure III-22: displaying the pathlines.....	46
Figure III.23: Saving files.....	47
Figure IV- 1: Mesh size independence on results, for (AR=0.2,0.4,0.6,0.8), $\phi=0.1$, $Ra = 10^6$ for water-cu.....	49
Figure IV- 2: The chosen mesh.....	50
Figure IV- 3: I- Mahmodi et Seyed [28] Streamlines (up) and isotherms (down) inside the C-shaped enclosure filled with pure fluid ($\phi=0$) at $Ra=10^6$, (a) AR=0.2, (b) AR =0.4, (c)AR=0.6, (d)AR=0.8[28]. II present study.....	51

Figure IV- 5: Comparison of Rayleigh number variation as a function of mean Nusselt number for ($\phi=0$); left figure: reference results (Mostafa Mahmoodi and Seyed Mohammad Hashemi [28]); right figure: our result.....**52**

Figure IV- 6: Isotherms inside the cavity with AR=0.2 for pure fluid (up) and nanofluid water-cu with $\phi=0.1$ (down), (A) $Ra=10^3$, (B) $Ra=10^4$, (C) $Ra=10^5$, (D) $Ra=10^6$**53**

Figure IV- 7: Streamlines inside the cavity with AR=0.2 for pure fluid (up) and nanofluid water-cu with $\phi=0.1$ (down), (A) $Ra=10^3$, (B) $Ra=10^4$, (C) $Ra=10^5$, (D) $Ra=10^6$**53**

Figure IV- 8: Rayleigh number variation as a function of average Nusselt number for AR=0.2.....**54**

Figure IV- 9 V-velocity with AR=0.2, ($\phi=0.1$) water-cu.....**54**

Figure IV- 10: Streamlines (down) and isotherms (up) inside the C-shaped enclosure filled with nanofluid Water-TiO₂($\phi=0.1$) at AR=0.2, (A) $Ra=10^3$, (B) $Ra=10^4$, (C) $Ra=10^5$, (D) $Ra=10^6$**57**

Figure IV- 11: Rayleigh number variation as a function of average Nusselt number for AR=0.2 water-TiO₂.....**57**

Figure IV- 12 V-velocity with AR=0.2, ($\phi=0.1$) water-TiO₂.....**58**

Figure IV- 13: Streamlines (down) and isotherms (up) inside the C-shaped enclosure filled with nanofluid water-cu ($\phi=0.1$) at $Ra=10^6$, (A) AR=0.2, (B) AR=0.4, (C) AR=0.6, (D)AR=0.8.....**60**

Figure IV- 14: average Nusselt number variation as a function of aspect ratio for ($\phi=0.1$, $RA=10^6$) water-cu.....**60**

Figure IV- 15 V-velocity with $RA=10^6$, ($\phi=0.1$) water-cu.....**61**

Figure IV- 16: Streamlines (down) and isotherms (up) inside the C-shaped enclosure filled with nanofluid water-TiO₂ ($\phi=0.1$) at $Ra=10^6$, (A) $AR=0.2$, (B) $AR=0.4$, (C) $AR =0.6$, (D) $AR=0.8$**62**

Figure IV- 17: average Nusselt number as a function of aspect ratio number for ($\phi=0.1$, $RA=10^6$).....**63**

Figure IV- 18 V-velocity with $RA=10^6$, ($\phi=0.1$) water-TiO₂.....**63**

Figure IV- 19: Variation of average Nusselt number with nanoparticles volume fraction for different aspect ratios of enclosure filled with nanofluid water-cu, (a) $Ra=10^3$, (b) $Ra=10^4$, (c) $Ra=10^5$, (d) $Ra=10^6$**64**

Figure IV- 20 V-velocity with $RA=10^6$, $AR=0.2$ fot water-cu.....**65**

Figure IV- 21: Variation of average Nusselt number with nanoparticles volume fraction for different aspect ratios of enclosure filled with nanofluid water- TiO₂, (a) $Ra=10^3$, (b) $Ra=10^4$, (c) $Ra=10^5$, (d) $Ra=10^6$**66**

Figure IV- 22 V-velocity with $RA=10^6$, $AR=0.2$ for water-TiO₂.....**67**

General introduction:

Heat transfer is a very important process in industry and technology. Although it manifests itself in various forms (radiation, conduction and convection), the convection is the most common in some specific energy fields such as cooling of processors and electronic components, radiators and heat exchangers, solar thermal collectors, desalination, etc. [1]

Considering the forces, which produce the movement of the fluid, there are two types of convection: natural and forced convection. Natural (or free) convection differs from forced convection in that the movement of the fluid is not due to an external input of mechanical energy, but originates within the fluid itself, through the combined effect of mass volume gradients due to a temperature gradient [2].

In many engineering and process applications, which occur naturally, natural convection plays an important role as the dominant mechanism. In confined cavities, this phenomenon has received intensive attention in recent years, in view of the thermal performance of engineering and various scientific applications such as nuclear reactor systems, energy storage and conservation, cooling...etc. [3].

The base fluid used has a low thermal conductivity, which limits the improvement of heat transfer. However, the continued miniaturization of electronic devices requires further improvements in heat transfer. In an effort to save energy, an innovative technique using a mixture of nanoparticles with the base fluid was first introduced by Choi (S.U.S. Choi (1995)) [4]. The resulting mixture of the fluid and nanoparticles has unique basic physical and chemical properties. It is referred to as a nanofluid. It is expected that the presence of nanoparticles in the nanofluid

General introduction:

increases its thermal conductivity and significantly improves its heat transfer characteristics.

The improvement of heat transfer by natural convection is the main focus of several works, and to do so, a large number of researchers have carried out a multitude of numerical simulations and experimental tests on the description of the phenomena governing the phenomenon. The effect of the geometrical systems in which it takes place, and the physico-chemical properties of the fluids involved are examined.

Several geometrical configurations, more or less complex, have been examined under theoretical, numerical or experimental approaches in order to study, understand and improve the heat transfer [5]. In the present study, we present the case of a C-shaped cavity filled with nanofluid and subjected to a temperature gradient. This type of cavity is found in many industrial fields, especially during the cooling of electronic equipment and components.

In order to solve heat transfer problems, numerical methods must be used in cases where analytical solutions are not possible. The most commonly used numerical methods are: the finite difference method, the finite element method, and the finite volume method.

Each method has advantages and disadvantages, the most used method in the case of fluid mechanics and heat transfer is the finite volume method. Since this method has been chosen in most of the free or commercial CFD (Computational Fluid Dynamics) software, such as: COMSOL, StarCCM+, OpenFOAM, ANSYS CFX, ANSYS FLUENT...etc. In this work the commercial software ANSYS Fluent (2016) was chosen to solve the dynamic and thermal phenomenon studied

General introduction:

This thesis is divided into four chapters, as listed below:

- The first chapter presents a general overview and bibliographical study of natural convection in cavities in the presence of nanofluid numerically.
- The second chapter presents the configuration studied and the mathematical model adopted, as well as the associated boundary conditions.
- The third chapter presents the numerical simulation.
- The fourth chapter is dedicated to validation of the results, the analysis and comments of the different results of the simulations performed. Finally, a general conclusion summarizing the main results obtained during this study as well as some perspective are given.

Chapter I:

*GENERAL BACKGROUND AND
BIBLIOGRAPHICAL STUDY*

I-1 General background of heat transfer:

I-1-1 Introduction:

Heat transfer theory is a science, which studies the way, in which heat spreads from one region to another, under the influence of a temperature difference. Heat transfer is frequently encountered in nature and in various industrial systems. It results from a complex interaction within a medium or between media as soon as there is a temperature gradient. This interaction is responsible for the diversity of the resulting flows. Convection is composed of the three modes of heat transfer (conduction, convection, radiation) which is of vital importance in both fundamental and industrial fields such as: cooling of electronic components, air-conditioning, heat exchangers, nuclear power plants, solar panels, etc.

I-1-2 Definitions:

Heat transfer is the science that seeks to study the transfer of energy that can take place between material bodies due to a difference in temperature, the three modes of heat transfer are [6]:

- conduction
- convection
- radiation

I-2 Heat transfer:

Heat transfer is the science that attempts to predict the transfer of energy between molecules or particles of matter at different temperatures. The aim is to explain the manner and predict the rate of heat exchange under certain specific conditions. It complements the first two principles of thermodynamics with additional experimental laws to establish the proportions of energy transfer.

Heat transfer can be defined as the transmission of energy from one region to another once the temperature difference between them is established. It is governed by a combination of physical laws and empirical relationships deduced from experimentation. In the heat transfer literature, three distinct modes of heat transfer are generally recognized: conduction, convection and radiation [7].

I-2-1 Conductive heat transfer:

Thermal conductivity is the propagation of heat from molecule to molecule, in a body or in several contiguous and non-reflective bodies, without the movement of the fluid or the movement of the fluid being involved in the transmission. This mode of transmission characterizes mainly heat transfer in solids or between contiguous solid bodies. Conduction also occurs in liquids and gases, but except in the case of highly viscous liquids or gases trapped in a porous material, its effect is negligible compared to that of convection [8].

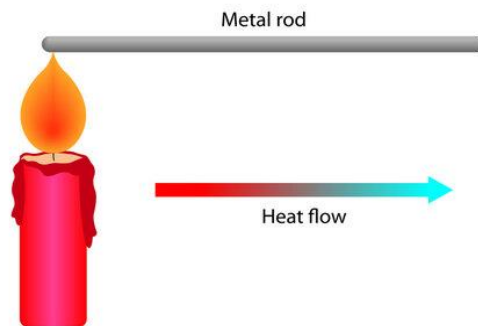


Figure I-1 Principle of heat conduction [29].

I-2-2 Radiant heat transfer:

This mode of heat transfer takes place by emission of electromagnetic waves, in all directions and belongs to the infrared and visible range. The radiation exchange is a mode of heat exchange that does not require a material support to propagate and

represents the only possibility of heat exchange between distant bodies placed even in a void, such as the heat exchange that is carried out between the sun and the earth [8].

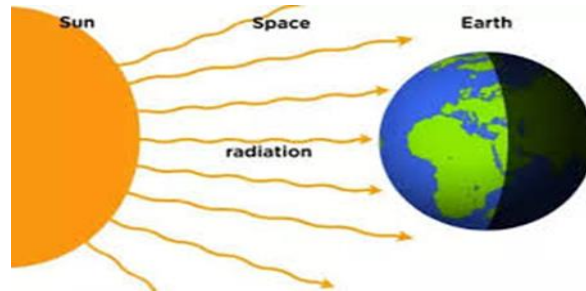


Figure I-2: Principle of radiation heat transfer[29].

I-2-3 Heat transfer by convection :

It is a transfer that results from an ensemble movement of the material supporting it. Convection therefore takes place in fluids (gases or liquids). It characterizes heat exchange at the boundary between a solid and a fluid and is therefore very much related to fluid flow but also to boundary geometries and solid surface states. A distinction must be made between forced convection, in which the fluid is set in motion by an external mechanical energy input (pump, fan, etc.), and natural convection, in which the fluid takes the energy necessary for movement from within itself (e.g. a variation in density associated with a temperature variation). Macroscopically, it is described by Newton's law (1701) which links the flow to a temperature difference [9].

$$\Phi = h \cdot S(T_p - T_f) \quad (1.1)$$

With:

Φ : Convective heat flux (W).

h: Convective heat transfer coefficient ($W \cdot m^{-2} \cdot C^{-1}$).

T_p : Surface temperature of the solid ($^{\circ}C$).

T_f : Temperature of the fluid away far from the solid surface ($^{\circ}C$).

S: Area of solid/fluid contact surface (m^2).

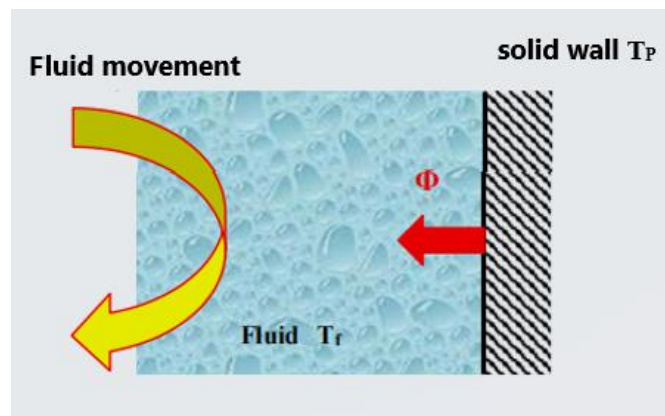


Figure I-3: Action of moving fluid in convection[29].

I-2-3-1 Different types of convection:

a) Forced convection:

Forced convection in which the movement is caused by a mechanical process independent of thermal phenomena, i.e. it is an external pressure gradient that causes the movement of the fluid particles. The study of heat transfer by convection is therefore closely linked to that of fluid flow.

Convection is said to be forced when there is a cause of the movement other than the temperature variations of the fluid, this cause being the only one to be considered because of its relative importance [10].



Figure I-4: The phenomenon of forced convection [29].

The general relationship for forced convection is

$$Nu = f(Re.Pr) \quad (1.2)$$

In microelectronics, the heat transfer then obeys the following expression:

$$Nu = C.Re^n.Pr^m \quad (1.3)$$

Where: C, n and m are constants which depend on the characteristics of the solid and the Fluid [10].

b) Natural convection

This is the one in which the movement of the fluid is created by differences in density, which are due to differences in temperature in the fluid.

Natural convection in which the movement results from the variation of the density of the fluid with the temperature; this variation creates a field of gravitational forces which conditions the movements of the fluid particles. Natural convection is due to the contact of the fluid with a hotter or colder wall, which creates differences in density that generate movement within the fluid.

This mode of heat transfer is found in several industrial applications, for example, in heat exchangers where two moving fluids, separated by a solid wall, exchange energy [11].

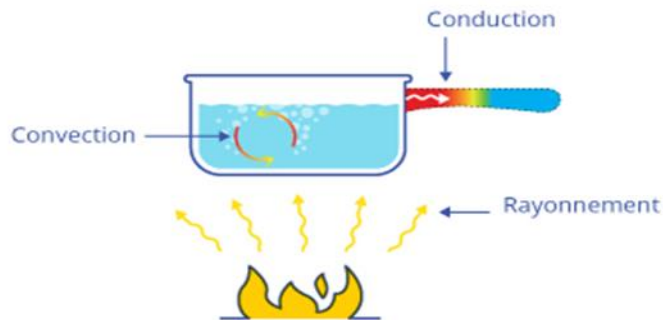


Figure I-5: Presentation of convection in a pan [29].

c) Mixed convection:

Corresponds to the coupling of the two previous modes of fluid movement resulting from the combination of forced and natural convection. The Richardson number Ri is the dimensionless group that determines which of these convections is dominant. Mixed convection can be aided (favorable) when the effects of natural convection (gravity) and forced convection (forced movement) are in the same direction. It is said to be counteracted (unfavorable) when these effects are in opposite directions.

* If the effects of gravity movement are opposed to forced movement, the flow is slowed down,

the heat transfer tends to decrease and we speak of "counteracted" mixed convection.

* If the forced flow is in the same direction as the free flow, there is an amplification of the transfers compared to the forced convection alone and we call it "assisted" mixed convection [12].

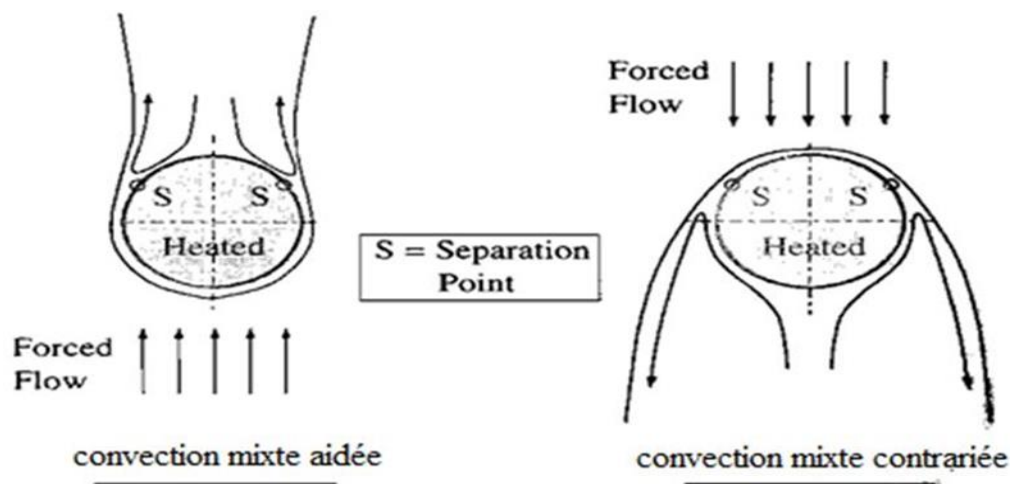


Figure I-6: Mixed convection, assisted [12].

I-3 The Dimensionless Numbers:

We will present the expressions and physical meaning of some dimensionless groupings that will be used throughout this work.

1- Number of Prandtl:

This is a dimensionless number proportional to the ratio of momentum diffusivity to thermal diffusivity. It characterizes the relative importance of thermal and viscous effects and is given by :

$$Pr = \frac{\nu}{\alpha} \quad (1.5)$$

With:

α : the thermal diffusivity [m^2/s]

The Prandtl number can also be written as:

$$Pr = \frac{\mu c_p}{K} \quad (1.6)$$

With:

C_p : specific heat of the mass at constant pressure [$J/kg.k$].

2- Number of Grashof:

The Grashof number is used to define the ratio between the forces of thrust (Archimedes) and the forces of inertia acting on a fluid and is expressed as follows:

$$Gr = \frac{g\beta L^3(T_P - T_{ext})}{\nu^2} \quad (1.7)$$

With:

g : the acceleration of gravity [m/s^2]

β : the coefficient of thermal expansion [1/k]

T_p : the temperature at the walls

T_{ext} : the external temperature.

3- Rayleigh number:

This is the ratio of the driving forces of the fluid ("Archimedes force") to the friction forces. The combined Prandtl and Grashof numbers are given by:

$$Ra = \frac{g\beta_f(T_h - T_c)H^3}{\alpha_f\nu_f} \quad (1.8)$$

4- Nusselt number:

The Nusselt number represents the ratio of convective to conductive heat transfer and is given by:

$$Nu = h \frac{L_f}{K_f} \quad (1.9)$$

With:

L_f : the length along which the flow takes place.

k_f : the conductivity of the fluid.

h : the heat exchange coefficient by convection.

I-4 Nanofluids

I-4-1 Definition of nanofluid:

Nanofluids are colloidal solutions composed of nanosized particles (nanoparticles) suspended in a liquid that is called a base liquid. The list of nanoparticles used to obtain nanofluids is very wide and includes [13]:

* aluminum, Al and aluminum oxide, Al₂O₃.

* copper, Cu and copper oxide, CuO.

* gold, Au.

* silver, Ag.

* carbon nanotubes.

* titanium dioxide, TiO₂.

The choice of base liquids is essential for a Nano-fluid, it ensures the stability of the suspension over time and avoids any aggregation phenomenon, the selection of such a fluid will depend on the nature of the nanoparticle, the most used solvents are:

* Water,

* Ethylene and propylene glycol,

* Oils and other lubricants,

* Toluene,

* Bio-fluids.

I-4-2 Types of nanoparticles:

Different types of nanomaterials have been used to prepare nanofluids, they can be classified into four categories:

- * Metal nanoparticles such as aluminum Al , copper Cu , iron Fe and silver Ag .
- * Ceramic oxide nanoparticles such as aluminum dioxide Al_2O_3 , copper oxide CuO , Titanium dioxide TiO_2 , zinc oxide ZnO and silicon dioxide SiO_2 .
- * Metal carbide nanoparticles such as metallic silicon carbide SiC .
- * Non-metallic nanoparticles such as graphite C and carbon nanotube CNT .

The best-known nanoparticles are shaped like:

- * Spherical,
- * Cylindrical,
- * Agglomerate.

The range of volume fractions studied in general is:

- * 0.1 - 1%
- * 1 - 10%
- * > 10%

I-4-3 Applications of nanofluids:

- Industry:

Since this allows us to reduce the size of cooling equipment or their electrical consumption without getting too tired, industry in general (heat engine, air conditioning, power portion, nuclear installation, particle accelerator, aeronautics or

space, etc.) may reduce the size of cooling equipment or their electrical consumption. Doubling the exchange coefficient would require a tenfold increase in pumping power, which would be enormous and uneconomic. By increasing this coefficient up to 80% under turbulent conditions without changing the power required for operation, a nanofluid can partially overcome this. [14].

-Cooling of electronic systems:

In the open cavity, nanofluids have been considered as cooling fluids, for this several studies have been carried out, Hamdi et al [15]. In the present work, the two-dimensional mixed convection fluid flow and heat transfer of water nanofluids (Cu, Ag, Al₂O₃ and TiO₂) in a two-sided lid-driven cavity partially heated from below were numerically studied. Two discrete heat sources are located on the bottom wall of the chamber; however, the vertical moving walls and the ceiling are cooled to a constant temperature. The remaining boundary parts of the bottom wall are kept insulated.

- Cooling of thermal systems:

Used mainly for cooling of energy systems and the effect of the form factor on the upward movement of fluid streams [16]. This point is studied by several groups of researchers, Bara et al [17], presented results of a natural convection of nanofluids in a closed cavity filled with pure water on the one hand and a mixture of water and nanoparticles (Cu) on the other hand for a varying Rayleigh number.

- Cooling of nuclear systems:

The Massachusetts Institute of Technology has set aside an interdisciplinary center solely for new nanotechnology (nanofluid) in the nuclear power industry. Currently, they are evaluating the potential impact of the use of nanofluids on neutron safety, and the economic performance of nuclear systems [18]. Boutra et al, [21], presented

results from the numerical study of the two-dimensional and planar flow and heat transfer in mixed convection mode within a square cavity, entirely filled with a nanofluid (Ag-water). The suspensions thus obtained can be used in a multitude of applications, such as the cooling of nuclear reactors, the optimization of heat transfer within a heat exchanger, etc.

- Other applications:

Fuel cell-solar water heating-domestic refrigerator coolers, Diesel combustion, Drilling, Lubricants, thermal storage [14] and heat pipes [19].

I-4-4 Advantages of Nano-fluids:

- * Large heat transfer surface between particles and fluids.
- * High dispersion and stability with predominantly Brownian motion of the particles.
- * Reduced heat transfer compared to pure liquid to obtain equivalent heat transfer intensification.
- * Reduced particle clogging compared to conventional slurries, allowing for miniaturization of the system.
- * Adjustable properties, including thermal conductivity and surface wettability, by varying particle concentrations for different applications

I-4-5 Disadvantages of Nano-fluids:

- * Lack of agreement of results obtained by different researchers.
- * Lack of theoretical understanding of the mechanisms responsible for changes in properties.
- * Poor characterization of suspensions.

CHAPTER I : GENERAL BACKGROUND AND BIBLIOGRAPHICAL STUDY

- * Stability of nanoparticles dispersion.
- * Increased pressure drop and pumping power.
- * Higher viscosity, lower specific heat.
- * High cost of Nano-fluids.
- * Difficulties in the production process [19].

I-5 BIBLIOGRAPHICAL STUDY

In recent years, several studies have been carried out on the convection of a nanofluid. This chapter is interested in presenting a bibliographical summary of some of the studies previously carried out and which are directly related to our case study.

I-5-1 Bibliographic summary :

The term "nanofluid" was first proposed by Choi [4] to refer to the suspension of solid nanoparticles in a base liquid. Choi [4] found that the effective thermal conductivity of the water-Al₂O₃ mixture increases by 20% for a volume concentration between 1% and 5% Al₂O₃

A significant amount of research has been carried out since 2001 on this new class of nanofluids in order to gain a better understanding of the mechanisms involved, and thus develop more efficient heat transfer fluids. The high thermal conductivity of nanofluids makes them potential candidates for replacing carrier fluids used in heat exchangers to improve their Koblinski performance [20]. Some limitations that could reduce the performance of nanofluids used instead of pure heat transfer fluids have been studied.

A. DAAS, S. DERFOUF, N. BELGHAR (2016) [21], made a numerical study of free convection in a rectangular geometry filled with a nano fluid (Cu/water) is heated by a thermal source. The continuity, mass and energy equations are discretized by the numerical finite volume method, using numerical simulation as a tool for investigation.

K. Najid, F. Dahami, Z. Boulahia and R. Sehaqui (2017) [22], presented a numerical study of natural convection in a nano-fluid (Cu/water) filled corrugated wall. Numerical simulation was used to design the code and the signal. They discretised

the decision equations by SOR and ADI methods. A parametric study was carried out considering the type of nano fluids, the ripple amplitude and the Rayleigh number. The results were analysed considering the Nusselt number through dynamic and thermal fields.

Ms. Tabet Sara (2017) [23], worked on a numerical study of natural convection in a laminar and turbulent regime inside a square shaped geometry with a partially heated wall. The heated part of the wall varies between 20% and 80% of the total length. The governing equations were solved by the finite difference method and the finite volume method.

Natural convection was shown in both laminar and turbulent states in the temperature and Nusselt curves. Partial heating has a significant impact on heat transfer. The Rayleigh number is larger when the effect is more intense, the Rayleigh number being between 10^6 - 10^9 in laminar and turbulent systems.

KROUMA Saadia, N. BELGHAR (2017) [24], have achieved through this numerical study a detailed analysis of thermal exchanges by nanofluids in order to understand and valorize the different mechanisms that prove to condition their thermophysical properties as well as their thermal improvements within a micro-heat exchanger intended for the cooling of electronic components.

M. El-Hattab et al [25] presented a numerical study of the natural convection of nanofluids confined in a square enclosure heated by an isothermal heat source mounted on its left wall. The equations governing the hydrodynamic flow and heat transfer are described by the Navier Stockes and energy equations. These equations are discretised by the finite volume method using a power law scheme. The dynamic viscosity and effective thermal conductivity of the nanofluid are approximated by the Brinkman and Maxwell-Garnetts models, respectively. The numerical

simulations are performed for pure water and mixtures of water and nanoparticles (Al_2O_3 , Cu and TiO_2) for a Rayleigh number varied between 10^3 and 10^6 and a volume fraction of nanoparticles between 0 and 0.1. The results obtained show that the heat transfer improves if the volume fraction of the nanoparticles and the Rayleigh number are increased.

S.M. Aminossadati, [26] performed a numerical analysis of the natural cooling of a heat source in the form of a right triangle by a nanofluid (water-CuO) in a right triangular cavity that is under the influence of a horizontal magnetic field. The effects of Rayleigh number, solid volume fraction, Hartmann number and the position of the heat source in the cavity on the heat transfer performance of the cavity are examined. The results show that the thermal performance of the cavity is increased when the Rayleigh number increases, the Hartmann number decreases and the distance of the heat source from the cold walls decreases. An optimal solid volume fraction is found that maximises heat transfer at high Rayleigh numbers.

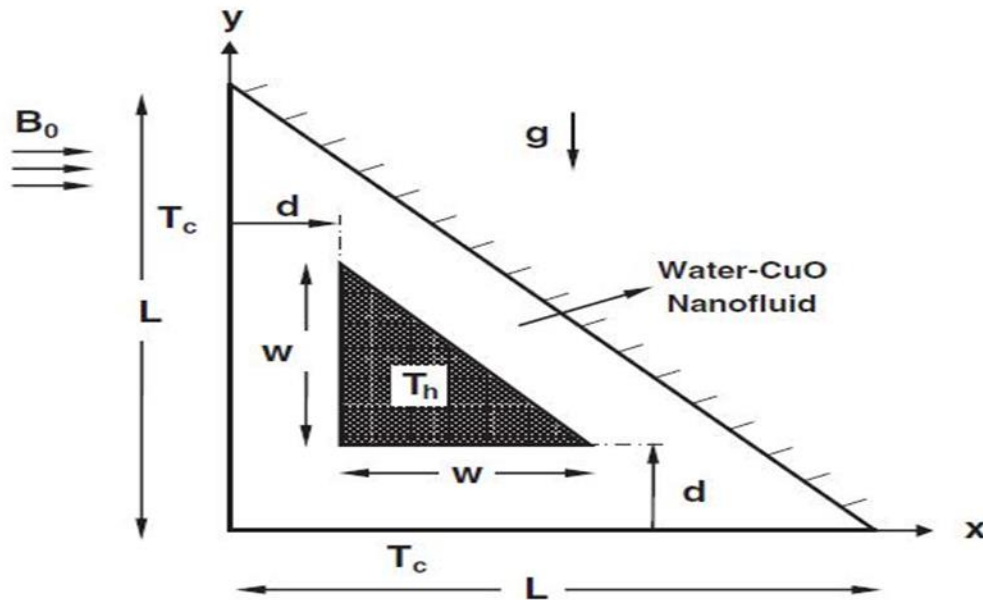


Figure 1- 7: Right triangular cavity containing a right triangular heat source under the influence of a magnetic field, study by S.M. Aminossadati [26].

A. Bouhelal et al [27] have numerically studied the natural convection cooling of an integrated heat source on the bottom wall of a square chamber filled with a water-copper nanofluid. The upper and vertical walls of the enclosure are kept at a relatively low temperature (Figure I-2). The transport equations for a Newtonian fluid are discretized by the finite volume method and solved numerically using the Ansys Fluent CFD software. The influence of relevant parameters such as Rayleigh number, heat source location, volume fraction of the nanofluid on the cooling performance was studied. The results indicate that the addition of nanoparticles to pure water improves its cooling performance especially at low Rayleigh numbers. The location of the heat source was found to significantly affect the maximum temperature of the heat source.

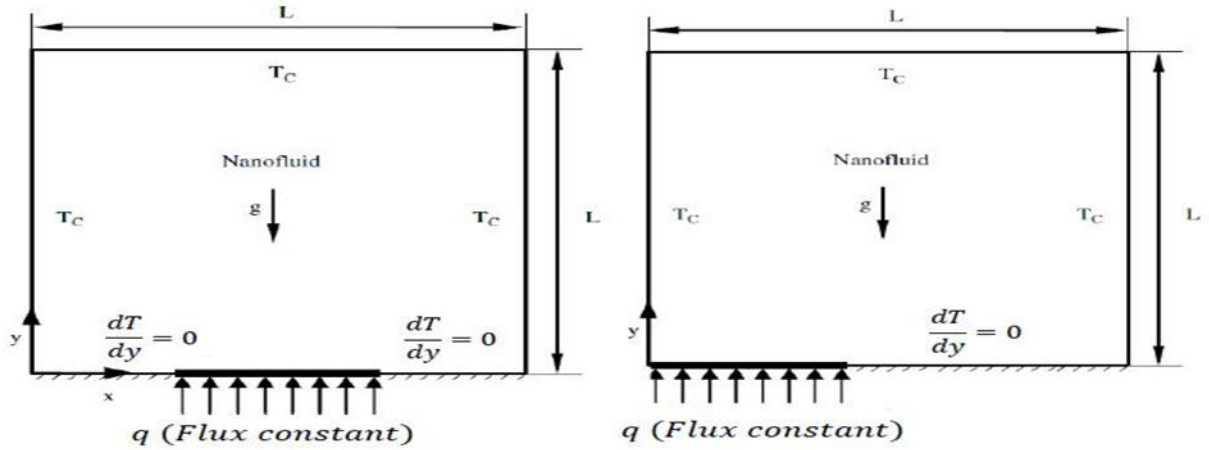


Figure 1- 8: Natural convection in a square cavity filled with nanofluid; geometrical description of the problem studied by A. Bouhelal et al [27].

S. Mojumder et al [3] studied the heat transfer by natural convection in a C-shaped enclosure filled with ferrofluid (Cobalt-Kerosene) in the presence of magnetic fields (Figure I-9). Various volume fractions between 0 and 0.15 were considered. Numerical simulations are performed for a wide range of Rayleigh number ($Ra = 10^3 \sim 10^7$) and Hartmann number ($Ha=0 \sim 100$). It was shown that the heat transfer rate is significantly improved for high Rayleigh numbers, while the presence of magnetic field attempts to retard the convection and then decrease the heat transfer. Furthermore, the addition of 15% nanoparticles to the base fluid can increase the heat transfer rate up to 52.65% for moderate Rayleigh numbers.

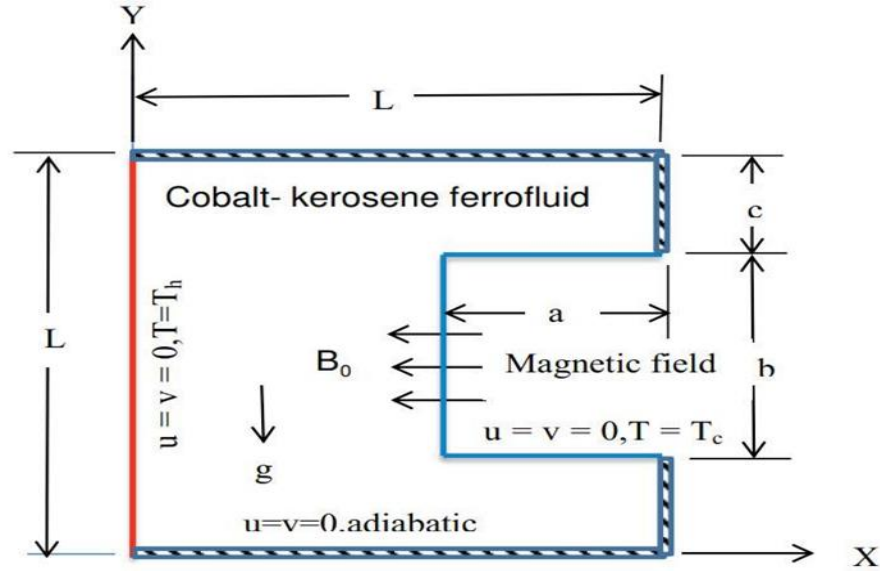


Figure 1- 9: Natural convection in a C-shaped cavity filled with ferrofluid; problem studied by S.Mojumder et al, [3]

Mostafa Mahmoodi and Seyed Mohammad Hashemi [28] conducted a numerical study of natural convection of a nanofluid in C-shaped enclosures. They investigated the effects of aspect ratio, Rayleigh number, and volume fraction of nanoparticles on heat transfer enhancement. They used the finite volume method to solve the governing equations in terms of primitive variables. They also defined dimensionless parameters to convert the governing equation to dimensionless form.

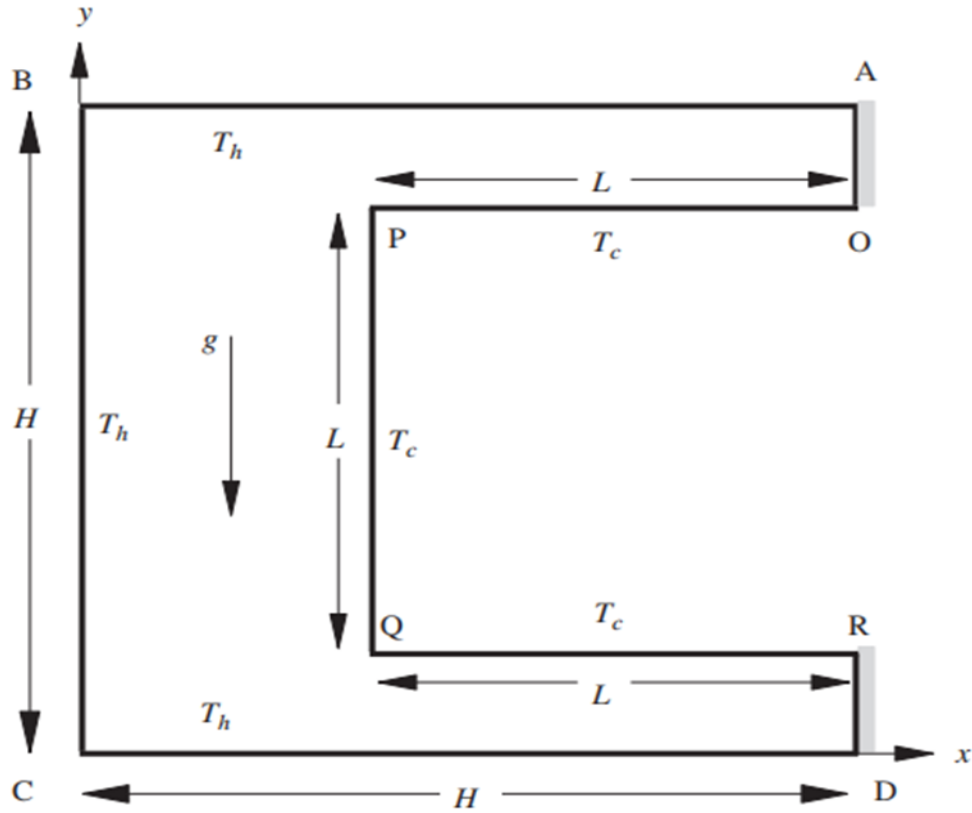


Figure. 1-10 A schematic view of the C-shaped enclosure considered in the present study [28]

In this work we are interested in numerically studying the heat transfer by natural convection in a C-shaped cavity in the presence of nanofluid. The dimensions of the cavity as well as the nanofluid used (water-cu) have been selected based on the work of Mahmoodi (2012). In the following chapter, the configuration and the mathematical formulation of the studied problem will be presented in detail.

Chapter II

Mathematical Modeling

II-1 Introduction :

The objective of this chapter is first to give the mathematical model governing the studied problem. First of all, we will present the geometrical configuration studied. Then, the governing equations, the working hypotheses and the thermophysical properties of the studied nanofluid will be discussed.

II-2 Mathematical modeling :

A schematic geometry of the C-shaped enclosure considered in the present study is shown in Fig.II-1. The top, left and bottom walls of the enclosure are kept at high temperature, T_h , and a cold square rid with temperature of T_c is located on the right adiabatic right wall of the enclosure which form a C-shaped enclosure. The adiabatic portions of the right wall are shown dashed. The height and the width of the cavity are noted H . The thickness of the enclosure is represented by L . The aspect ratio of the enclosure is defined as $AR = L/H$. The length of the cavity perpendicular to its plane is assumed to be long enough; hence the problem is considered two dimensional. The cavity is filled with Cu-water nanofluid. It is assumed that the nanoparticles and the base fluid are in thermal equilibrium and there is no slip between them. The thermophysical properties of nanoparticles and the water as the base fluid at $T = 25$ C are listed in Table 1. The nanofluid is considered Newtonian and incompressible and the nanofluid flow is assumed to be laminar. The thermophysical properties of the nanofluid are considered constant with the exception of the density which varies according to the Boussinesq approximation.

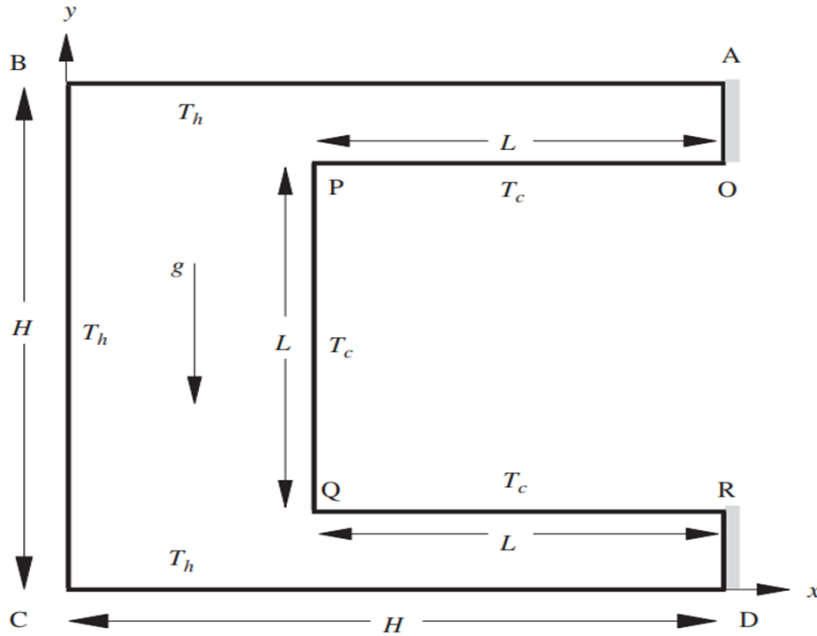


Fig. II-1. A schematic view of the C-shaped enclosure considered in the present study.

The equations governing steady state laminar free convection fluid flow and heat transfer are written below in terms of primitive variables. These equations are obtained after invoking Boussinesq approximation:

$$\frac{\partial u}{\partial x} + \frac{\partial v}{\partial y} = 0 \quad (2.1)$$

$$u \frac{\partial u}{\partial x} + v \frac{\partial v}{\partial y} = -\frac{1}{\rho_{nf}} \frac{\partial p}{\partial x} + \frac{\mu_{nf}}{\rho_{nf}} \left(\frac{\partial^2 u}{\partial x^2} + \frac{\partial^2 u}{\partial y^2} \right) \quad (2.2)$$

$$u \frac{\partial v}{\partial x} + v \frac{\partial v}{\partial y} = -\frac{1}{\rho_{nf}} \frac{\partial p}{\partial y} + \frac{\mu_{nf}}{\rho_{nf}} \left(\frac{\partial^2 v}{\partial x^2} + \frac{\partial^2 v}{\partial y^2} \right) + \frac{(\rho\beta)_{nf}}{\rho_{nf}} g(T - T_c) \quad (2.3)$$

And

$$u \frac{\partial T}{\partial x} + v \frac{\partial T}{\partial y} = \alpha_{nf} \left(\frac{\partial^2 T}{\partial x^2} + \frac{\partial^2 T}{\partial y^2} \right) \quad (2.4)$$

II-3 Thermophysical properties:

The thermo-physical properties of the nano-fluid used in this work, water-cu, water-TiO₂, are summarized in Table 1

Table 1: Thermophysical properties of water and solid nanoparticles.

Physical properties	Fluid phase	Cu	TiO ₂
CP (j/kg k)	4179	385	686.2
ρ (kg/m ³)	997.1	8933	4250
k (w/m.k)	0.613	401	8.9538
β(k ⁻¹)	21×10 ⁻⁵	1.67×10 ⁻⁵	0.9×10 ⁻⁵

The thermo-physical properties Cp, ρ, k and β are respectively the density, heat capacity, thermal conductivity and coefficient of thermal expansion.

$$\rho_{nf} = (1 - \varphi)\rho_f + \varphi\rho_s \quad (2.5)$$

$$(\rho Cp)_{nf} = (1 - \varphi)(\rho Cp)_f + \varphi(\rho Cp)_s \quad (2.6)$$

$$(\rho\beta)_{nf} = (1 - \varphi)(\rho\beta)_f + \varphi(\rho\beta)_s \quad (2.7)$$

And

$$\alpha_{nf} = \frac{K_{nf}}{(\rho Cp)_{nf}} \quad (2.8)$$

The thermal expansion coefficient of the nanofluid is calculated as follows :

$$\beta_{nf} = \frac{(1-\varphi)(\rho\beta)_f + \varphi(\rho\beta)_s}{(1-\varphi)\rho_f + \varphi\rho_s} \quad (2.9)$$

The Brinkman formula is employed to estimate effective dynamic viscosity of nanofluid:

$$\mu_{eff} = \frac{\mu_f}{(1-\phi)^{2.5}} \quad (2.10)$$

The effective thermal conductivity of the nanofluid is determined according to Maxwell:

$$\frac{K_{nf}}{K_f} = \frac{(K_s+2K_f)-2\phi(K_f-K_s)}{(K_f+2K_s)+\phi(K_f-K_s)} \quad (2.11)$$

II-4 Adimensionalization of equations :

The dimensionalities or normalization of equations consists in transforming the dependent and independent variables into dimensionless variables, i.e. they will be normalized with respect to some characteristic dimension. This allows to specify the flow conditions with a restricted number of parameters in order to make the solution more general.

In order to make the above equations dimensionless, they can be transformed by the following relations.

$$X = \frac{x}{H}, Y = \frac{y}{H}, U = \frac{uH}{\alpha_f}, V = \frac{vH}{\alpha_f}, P = \frac{pH^2}{\rho_{nf}\alpha_f^2}, \theta = \frac{T-T_c}{T_h-T_c} \quad (2.12)$$

The governing equations in dimensionless form are as follows:

$$\frac{\partial U}{\partial X} + \frac{\partial V}{\partial Y} = 0 \quad (2.13)$$

$$U \frac{\partial U}{\partial X} + V \frac{\partial U}{\partial Y} = -\frac{\partial P}{\partial X} + \frac{\mu_{nf}}{\rho_{nf}\alpha_f} \left(\frac{\partial^2 U}{\partial X^2} + \frac{\partial^2 U}{\partial Y^2} \right) \quad (2.14)$$

$$U \frac{\partial V}{\partial X} + V \frac{\partial V}{\partial Y} = -\frac{\partial P}{\partial Y} + \frac{\mu_{nf}}{\rho_{nf}\alpha_f} \left(\frac{\partial^2 V}{\partial X^2} + \frac{\partial^2 V}{\partial Y^2} \right) + \frac{(\rho\beta)_{nf}}{\rho_{nf}\beta_f} RaPr\theta \quad (2.15)$$

And

$$U \frac{\partial \theta}{\partial X} + V \frac{\partial \theta}{\partial Y} = \frac{\alpha_{nf}}{\alpha_f} \left(\frac{\partial^2 \theta}{\partial X^2} + \frac{\partial^2 \theta}{\partial Y^2} \right) \quad (2.16)$$

where the Rayleigh number Ra, and the Prandtl number Pr, are:

$$Ra = \frac{g\beta_f(T_h - T_c)H^3}{\alpha_f\nu_f}, Pr = \frac{\nu_f}{\alpha_f} \quad (2.17)$$

The boundary conditions for Eqs. (2.13) and (2.16) are:

$$\left\{ \begin{array}{l} \text{On walls AB, BC, CD: } U=V=0, \theta = 1 \\ \text{On walls OP, PQ, QR: } U=V=0, \theta = 0 \\ \text{On walls AO, DR: } U=V=0, \frac{\partial \theta}{\partial n} = 0 \end{array} \right. \quad (2.18)$$

where n is normal direction to the walls.

The local Nusselt number of the hot wall is:

$$Nu_{local} = \frac{hH}{K_f} \quad (2.19)$$

where the heat transfer coefficient, h, is:

$$h = \frac{q_w}{T_h - T_c} \quad (2.20)$$

The thermal conductivity is calculated as following:

$$\left\{ \begin{array}{l} \bullet K_{nf} = -\frac{q_w}{\partial T / \partial X} \text{ on wall BC} \\ \bullet K_{nf} = -\frac{q_w}{\partial T / \partial Y} \text{ on wall AB, CD} \end{array} \right. \quad (2.21)$$

CHAPTER II : Mathematical modeling

By substituting Eqs. (21) and (20) in Eq. (19), the Nusselt number can be written as:

$$\left\{ \begin{array}{l} \bullet \quad Nu_l = - \left(\frac{K_{nf}}{K_f} \right) \frac{\partial \theta}{\partial X} \text{ on wall } BC \\ \bullet \quad Nu_l = - \left(\frac{K_{nf}}{K_f} \right) \frac{\partial \theta}{\partial Y} \text{ on wall } AB, CD \end{array} \right. \quad (2.22)$$

The average Nusselt number of the hot wall is obtained by integrating the local Nusselt number along the hot walls as follows:

$$Nu = \frac{1}{3} \left(\int_0^1 Nu_l dX|_{y=0} + \int_0^1 Nu_l dY|_{x=0} + \int_0^1 Nu_l dX|_{y=1} \right) \quad (2.23)$$

Chapter III

Numerical

method

III-1 Introduction :

Over the years the development of computers has encouraged scientists to solve increasingly complex problems for which analytical solutions cannot be found. These types of problems are usually modelled by non-linear partial differential equations (PDE).

This chapter is dedicated to the modelling of flow and heat transfer. It covers the study of natural convection in a C-shaped enclosure with nanofluid, mainly using the ANSYS Workbench software, which is specially designed for computational fluid dynamics (CFD). CFD is a set of numerical methods for obtaining an approximate solution to problems in fluid dynamics and heat transfer. Numerical methods are used to solve the equations of fluid mechanics. The equations of continuity, momentum and energy are solved by the finite volume method, using the calculation code FLUENT.

III-2 Calculation procedures:

The Workbench is a software program that allows you to manage files and launch different programs from a single interface.

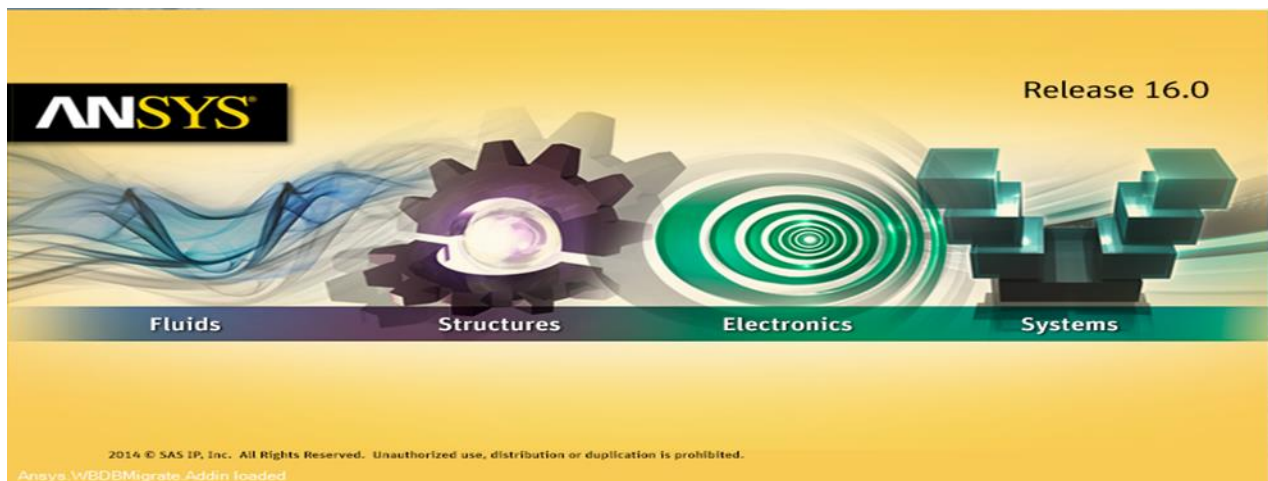


Figure III-1: Software launch window.

CHAPTER III : Numerical method

The general structure of the software is shown as follows:

ANSYS Workbench main menu:

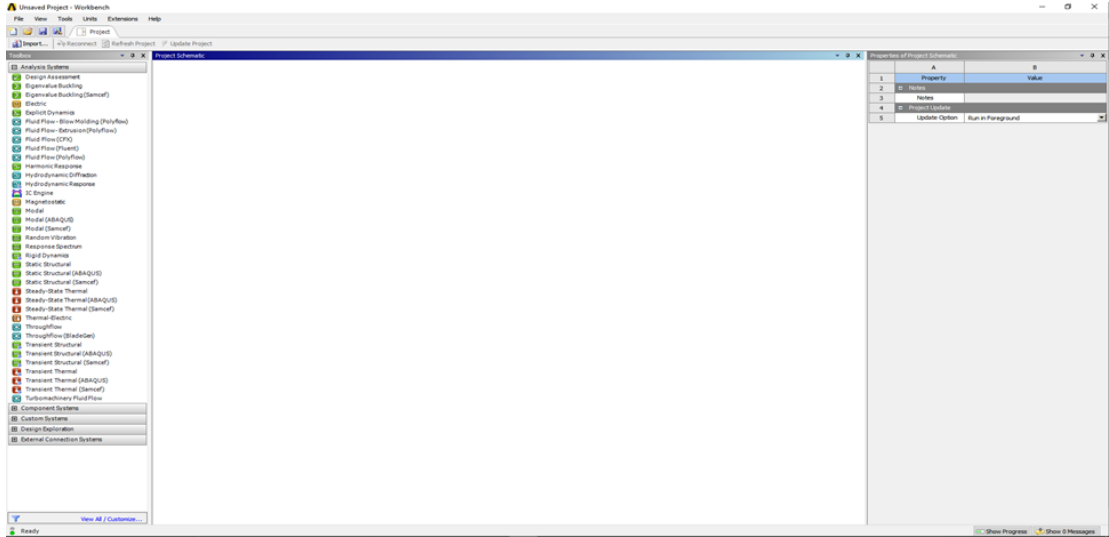


Figure III-2: Workbench main menu.

The opening of the software brings up the main menu below:

The toolbar gives access to several systems for analysis. To start dragging a fluid flow (fluent) analysis to the project scheme.

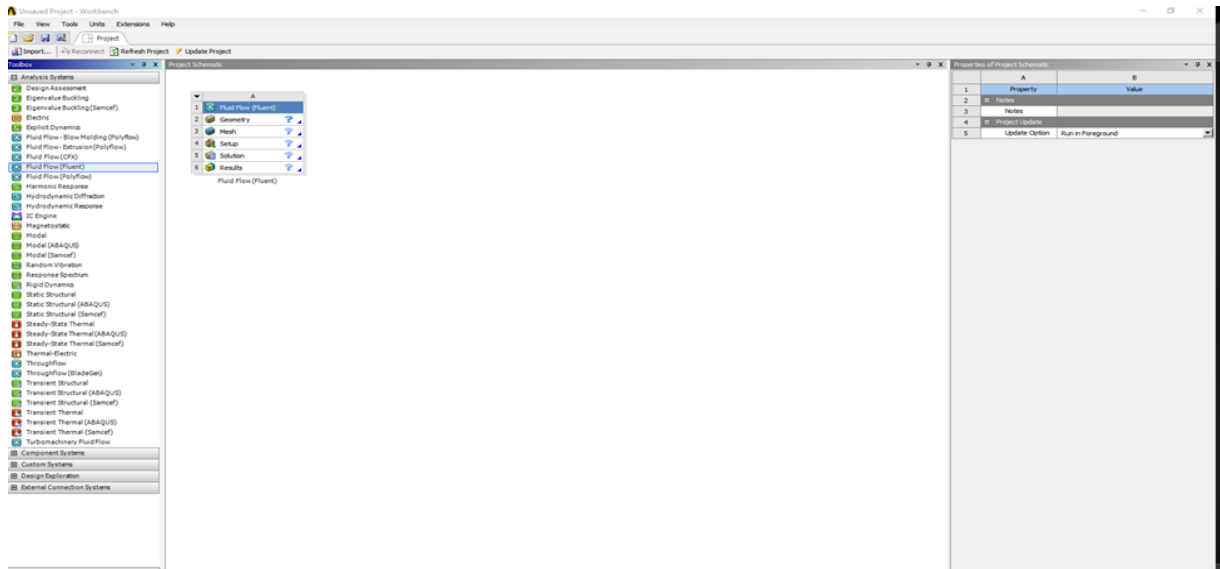


Figure III-3 Creating a fluid fluent (project)

The calculation steps are divided into 5 steps:

1. **Geometry:** used to import or create or modify or update a model that can be used for analysis.
2. **Mesh:** This cell is related to the definition of the geometry, coordinate systems and communication network and mesh in the mechanical simulation module, in addition to declaring certain physical properties of certain materials.
3. **Configuration:** allows to define loads and boundary conditions and another configuration for the analysis
4. **Solution:** this cell allows access to the solution data.
5. **Results:** This cell combines the results of the analysis.

III-3 Creation of the geometry:

To create a geometry with ANSYS Workbench double click on the geometry to open the geometry creation module "Design Modeler" figures: (IV.4), (IV.5).

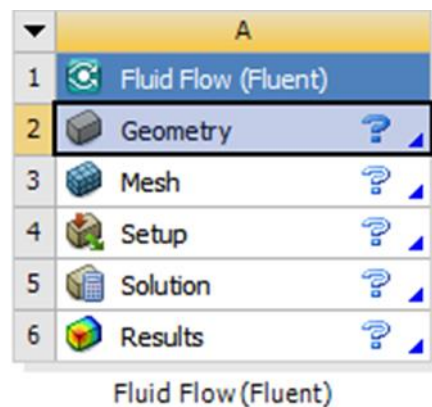


Figure III-4: fluid project project scheme.

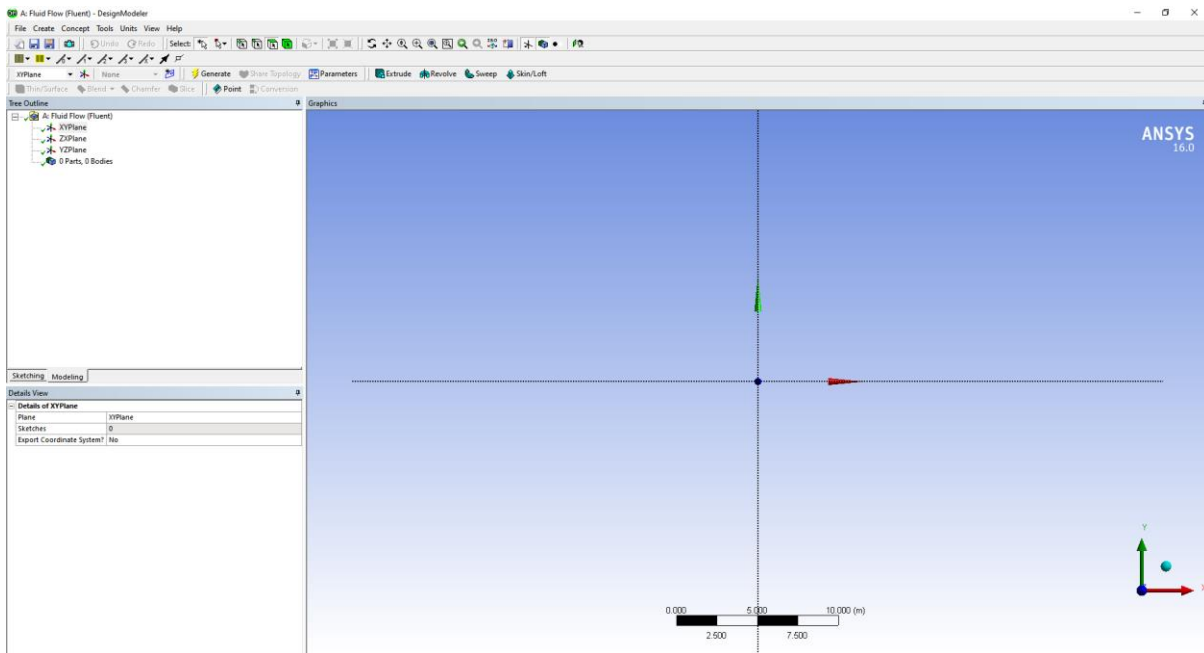


Figure III-5. Creating a geometric model (Design Modeler).

To draw the study geometry, click on the sketch toolbox, which will allow you to create the geometry, add dimensions and draw boundaries:

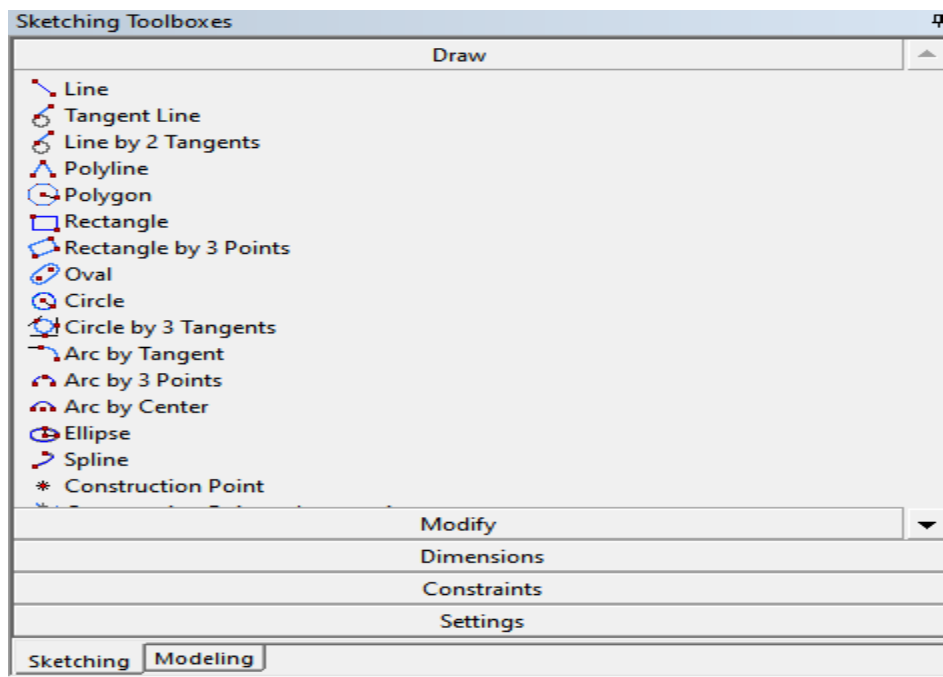


Figure III-6. Sketch creation.

CHAPTER III : Numerical method

In the Sketch toolbox we make the design in the plan we have chosen, then select the dimensions to the geometry as follows:

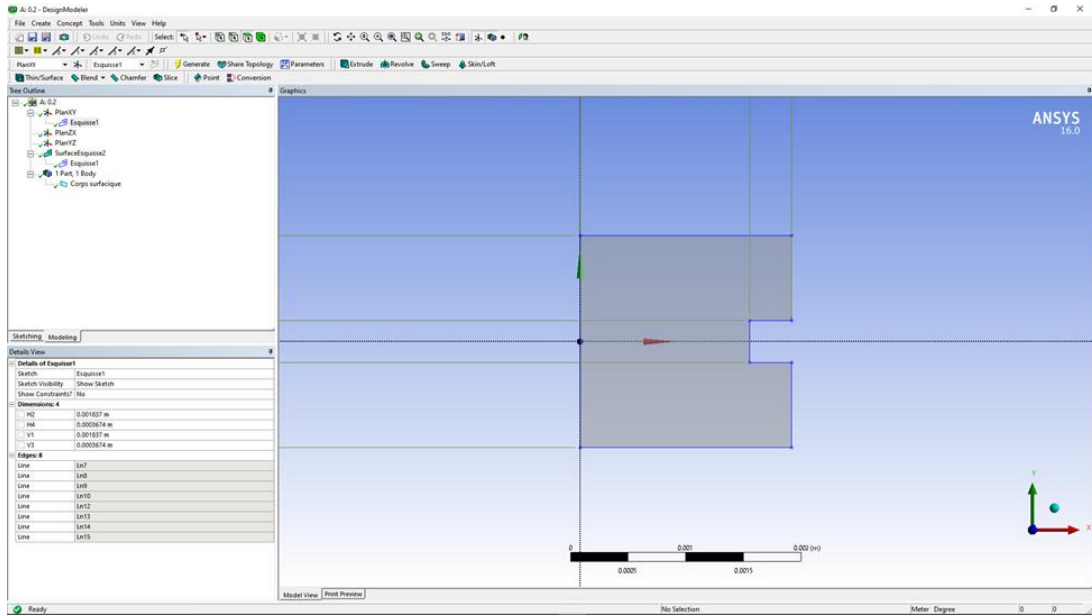


Figure III-7. Sketch creation

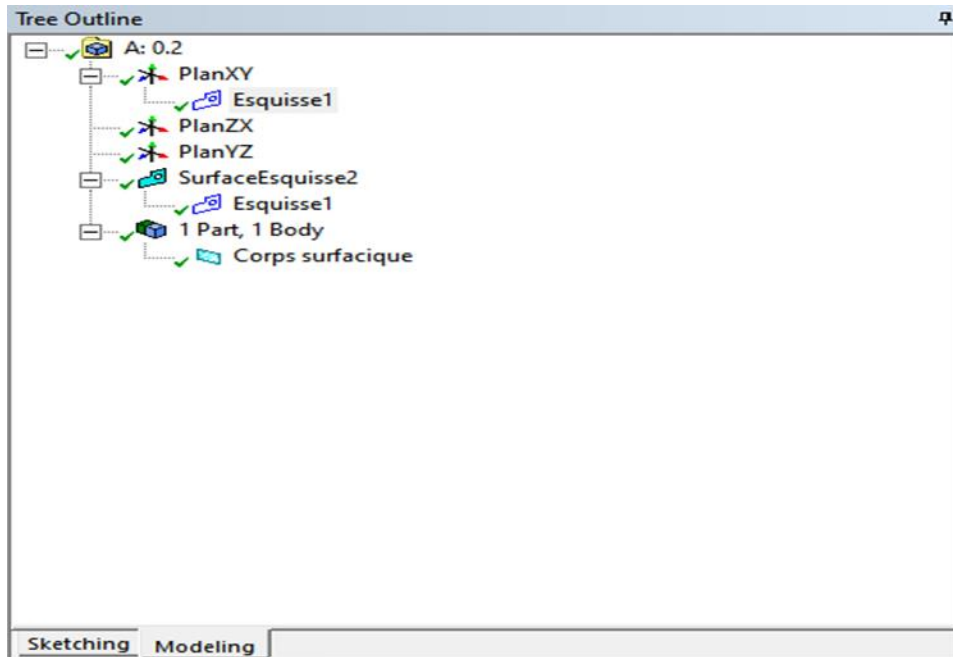


Figure III-8. Operation completed.

CHAPTER III : Numerical method

In the project scheme, after completing and finishing all operations, you will be notified that the creation in the design modeler was successful.

The option means that our geometry is ready for meshing.

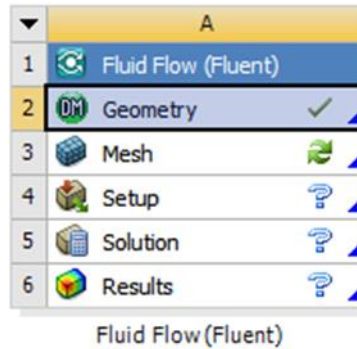


Figure III-9. Project scheme.

III-4 The mesh:

In the ANSYS Workbench project scheme, double-click on the mesh cell in the fluid mechanics analysis system.

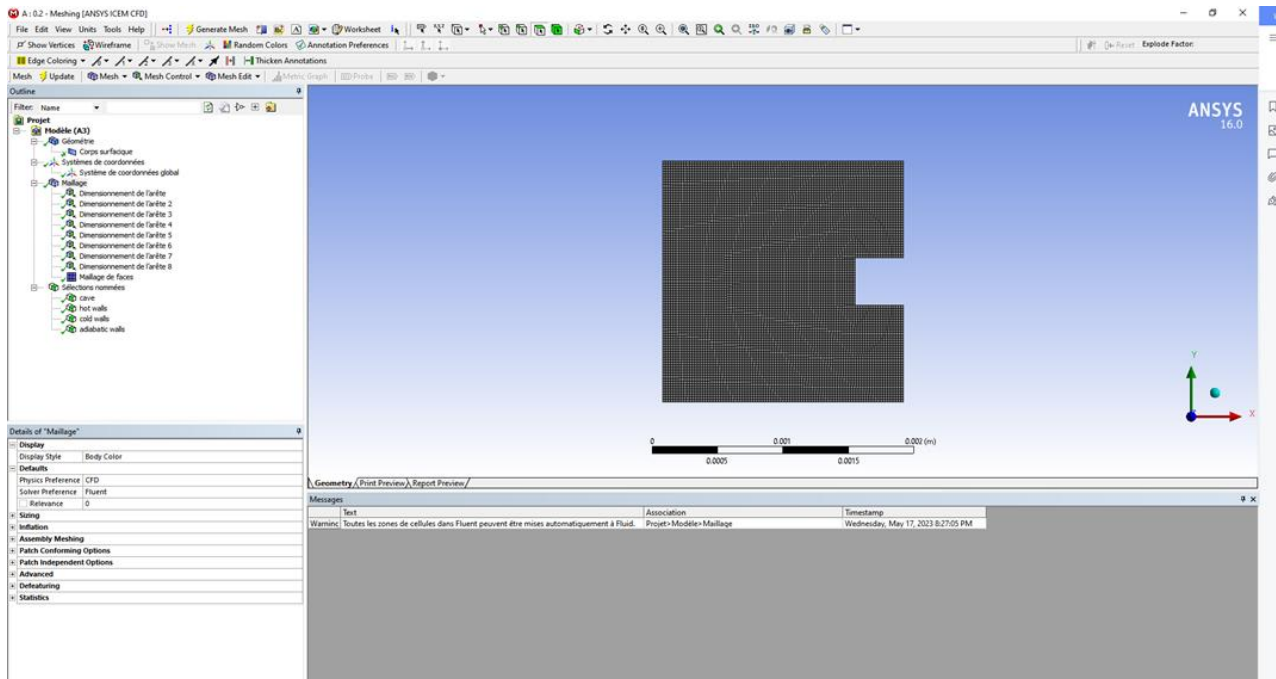






Figure III-10. Mesh.

CHAPTER III : Numerical method

- * In defining the boundary conditions of the geometry to simplify our work later in ANSYS Fluent, we must label each boundary in the geometry by creating named selections for the inputs, output and symmetry surface of the geometry. (Outer wall boundaries are automatically detected by ANSYS Fluent).
- * Select the large input to the geometry that is displayed in ANSYS mesh.
- * Right click and select the Create Named Selection option.
- * For each step of the named selection you must select the edge option 
- * Select the edge by clicking the right button. This operation is executable for all named selections of this problem: cold wall, hot wall, adiabatic wall.
- * To select the geometry of the space filled with nanofluid you have to click on face  then select area.
- * When the mark () appears on the mesh in the project diagram you can go to the next step which will be displayed by the mark ().
- * Save and exit the ANSYS workbench mesh and move on to the configuration and analysis on CFD in ANSYS Fluent.

III-5 Configuration:

In the ANSYS Workbench project scheme, double-click on the configuration setup cell in the fluid mechanics.

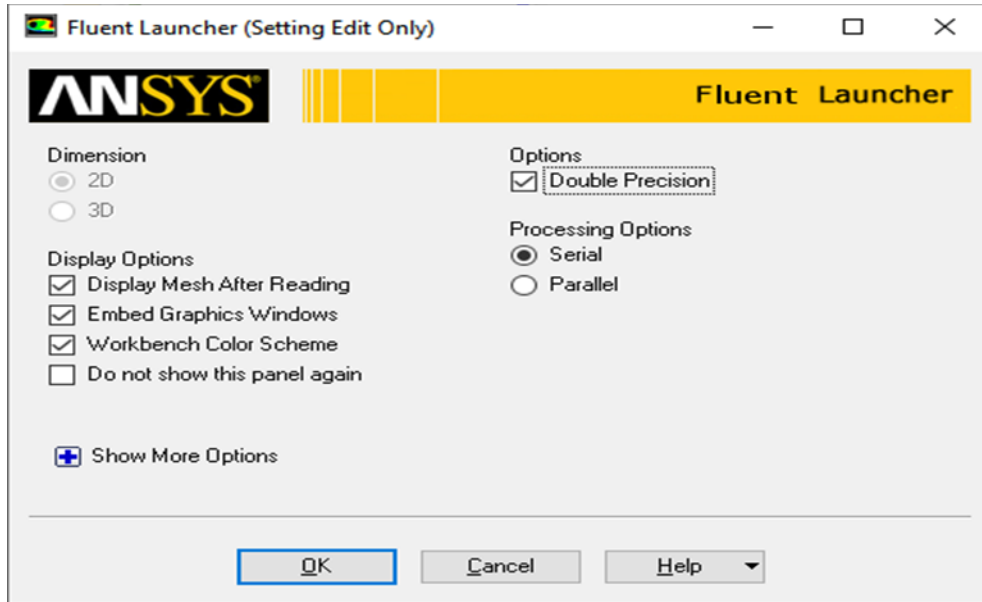


Figure III-11. Configuration of the simulation on fluent.

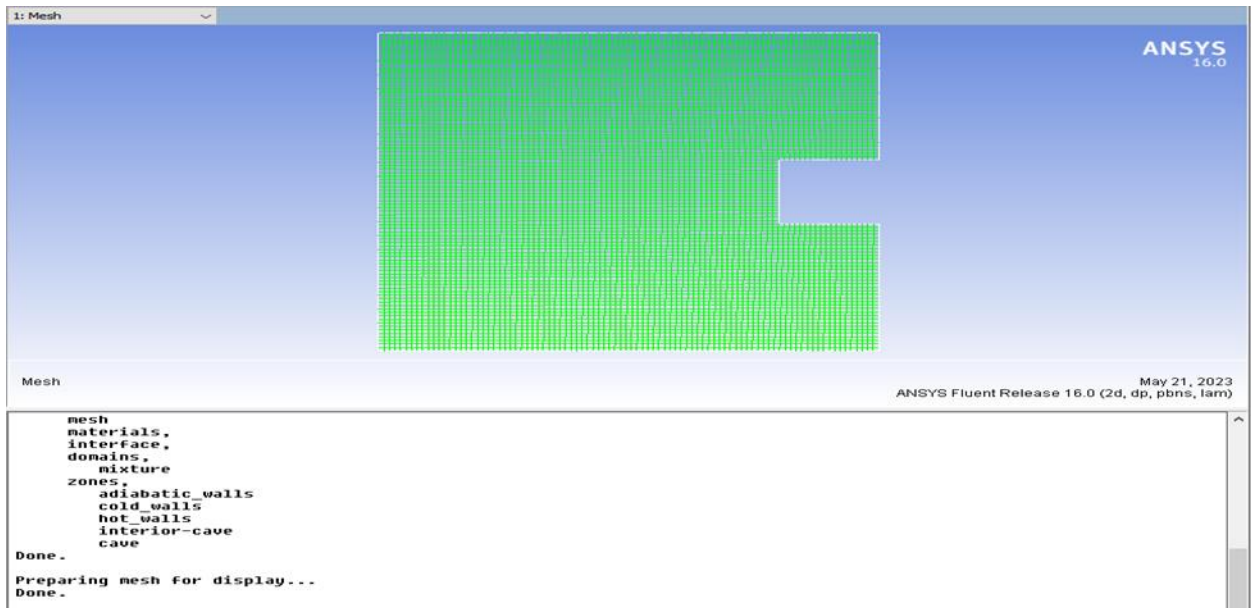


Figure III-12. ANSYS FLUENT.

a) Define the general parameters of the CFD analysis:

Click on General to open the general setup tasks page → General

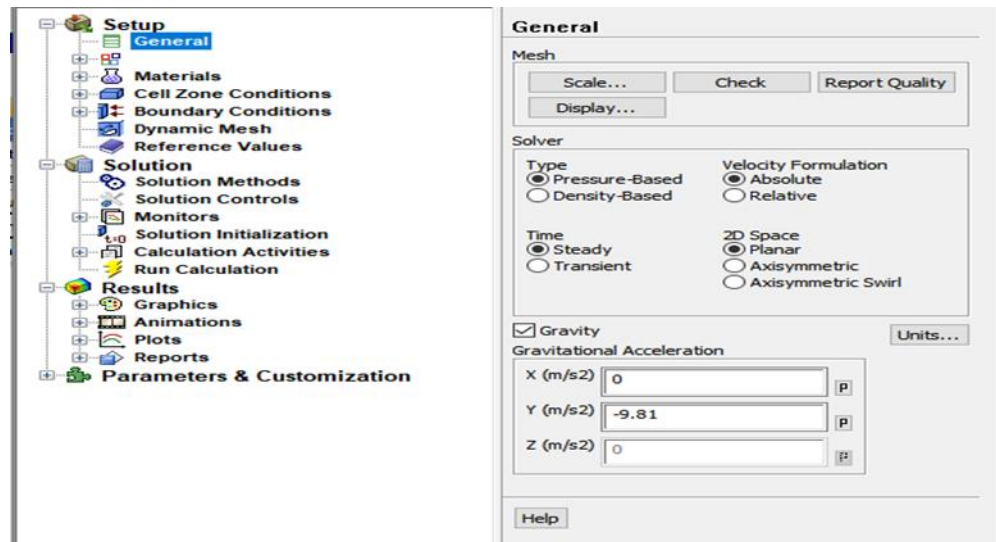


Figure III-13. General CFD parameters.

b) Setting the flow model:

The laminar flow model and the energy equation are specified using:

Setup → General

* Double click on Viscous- laminar and select Laminar.

* Double click on Energy and select Energy equation.

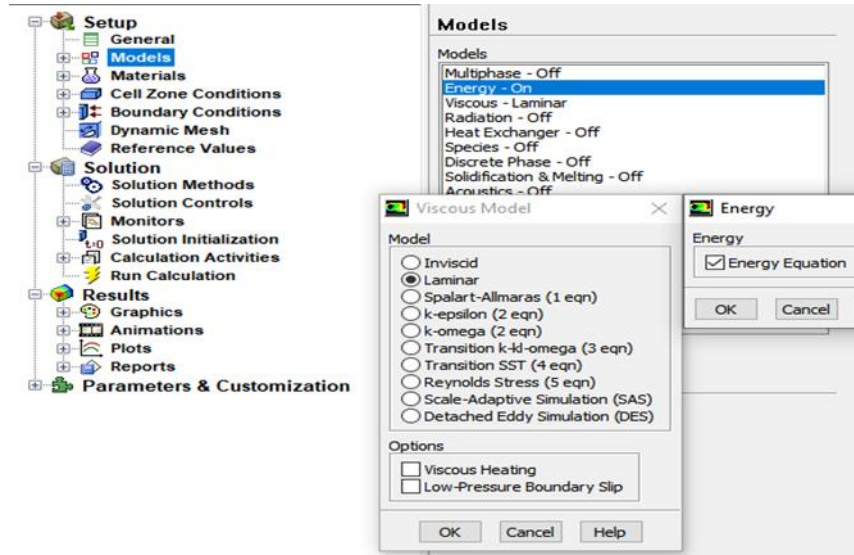


Figure III-14. Setup of the analysis model.

c) Materials :

- * The material is defined using setup → Materials.
- * Click on fluid to open the Create/EditMaterials window.
- * Click on fluent data base to select the fluid (materials).

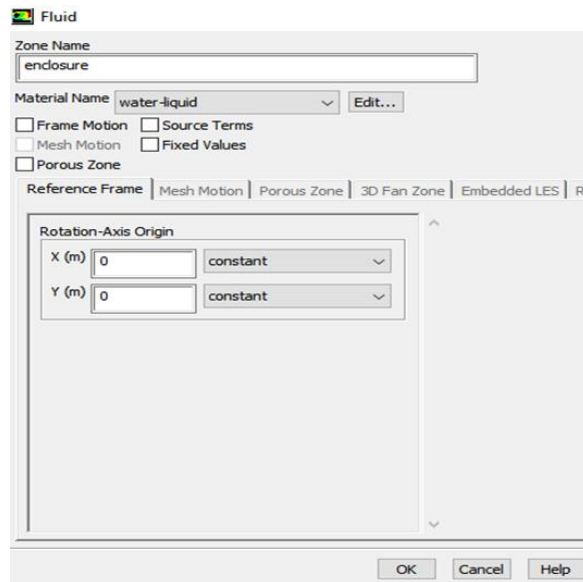


Figure III-15. Selection of fluid zone.

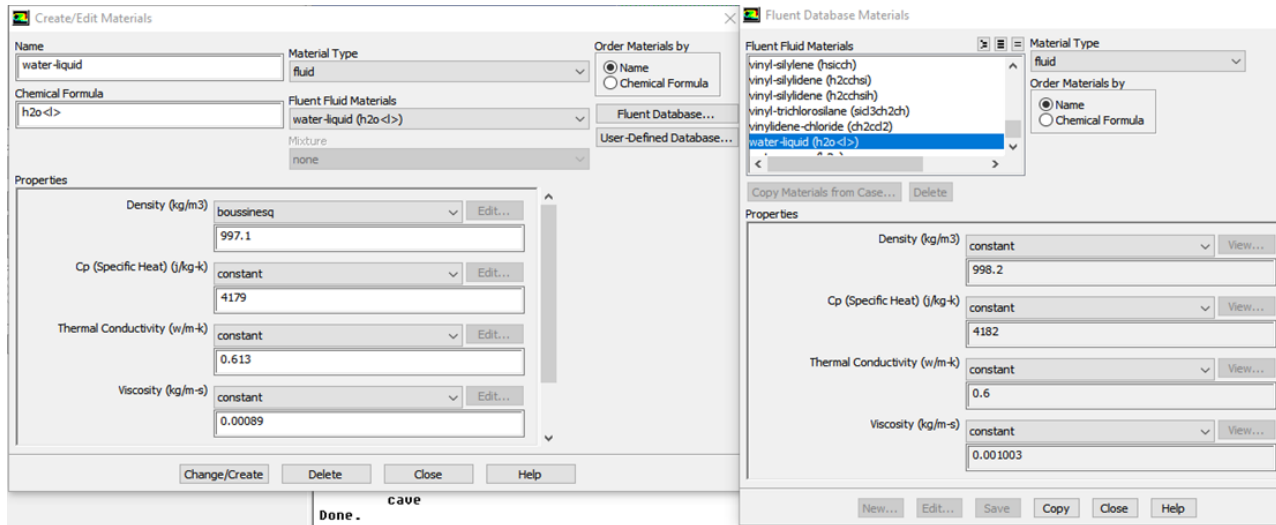


Figure III-16. Selection of materials.

* Click on copy.

* Change name, chemical formula, thermal and physical properties for each type of nanofluid.

* Click on Change/Create.

d) Setting up the cell area conditions for the CFD simulation:

We identified to nanofluid on the body surface:

* To change cell zone conditions using setup → cell zone conditions.

* Double-click on nanofluid and change material name.

e) Boundary conditions:

* To change the boundary conditions using setup → Boundary Condition.

* Double-click on the zone you want to change, we have identified the following boundary conditions:

* (cold wall): $T_c=20C$.

* The other walls (adiabatic wall) are thermally insulated and considered as adiabatic.

* (hot wall): $T_h=30C$.

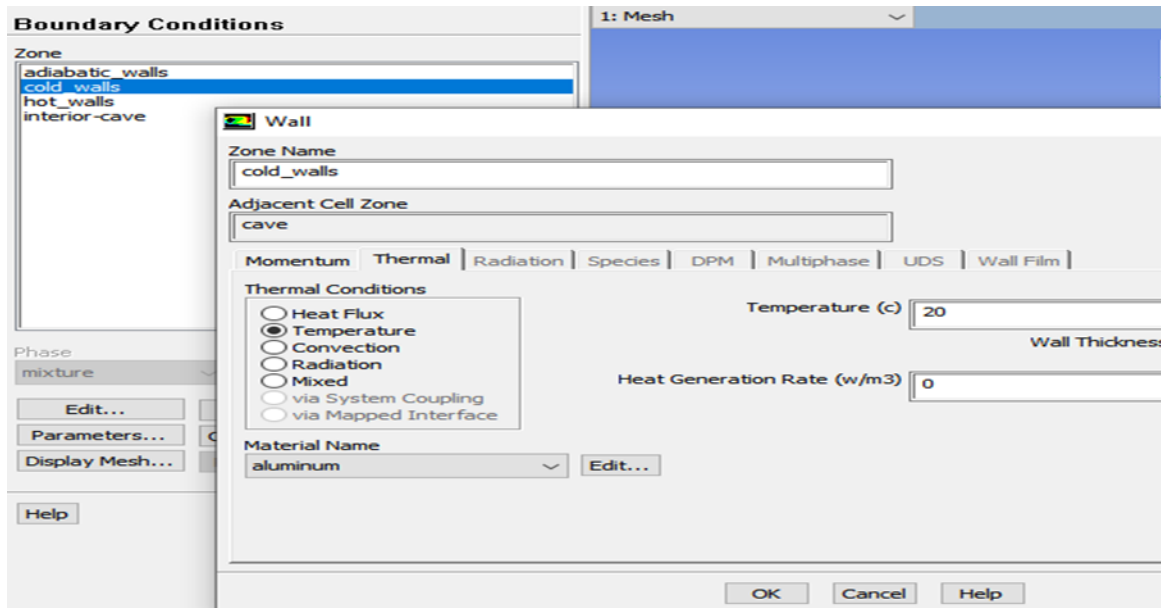


Figure III-17. Boundary condition.

f) Initializing the calculation:

setup → Solution Initialization → Initialize...

Initialize the flow field for the input value:

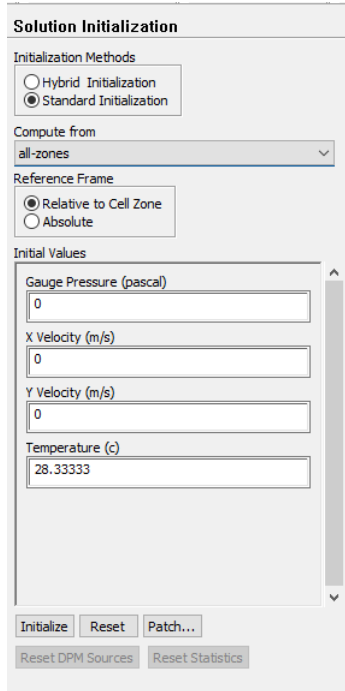


Figure III-18: Initialization of the solution.

g) Start calculation:

Setup → Run calculation ...

To begin the calculations, you must first choose the number of iterations.

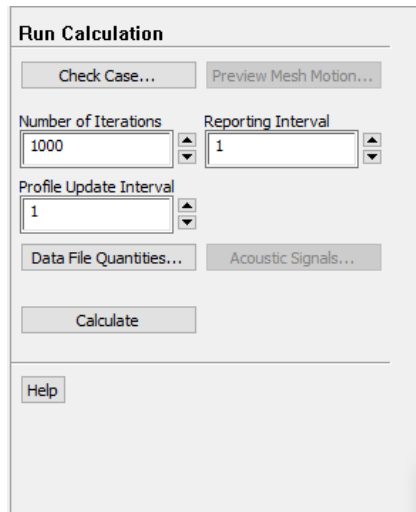


Figure III-19: Choosing the number of iterations

h) Evolution of calculation residuals:

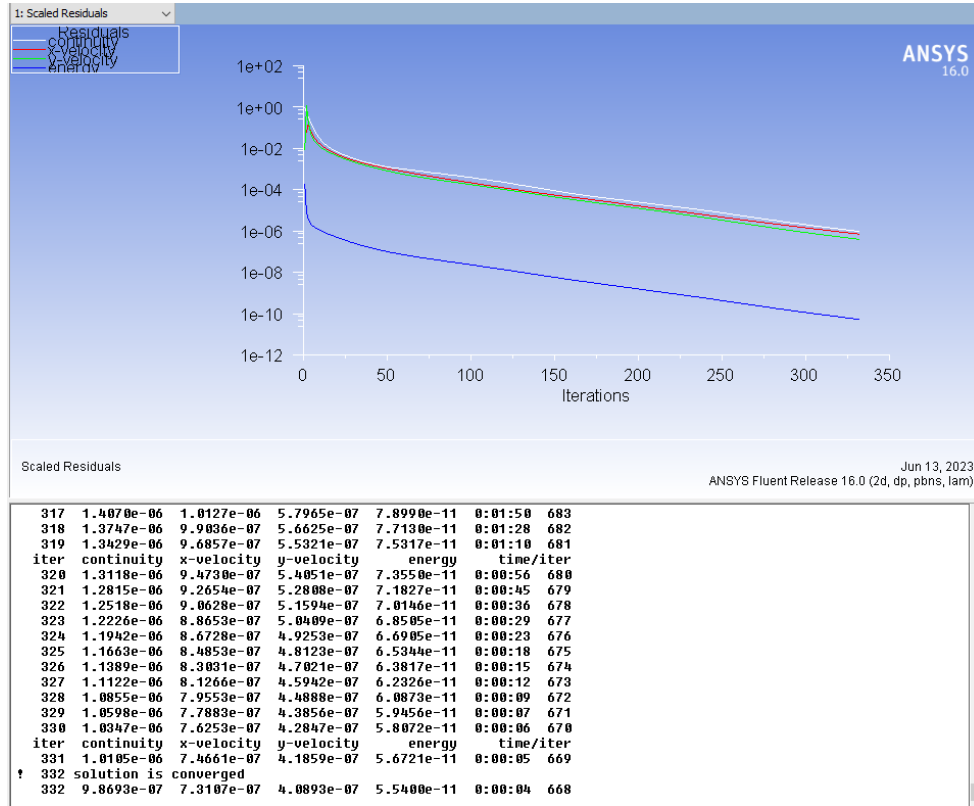


Figure III-20: Evolution of residuals for a cavity filled with nanofluid (Cu/water), $\phi = 0.01$, $Ra = 10^6$.

i) Visualization of the results:

Results → Graphics → Contours.

Results → Graphics → pathlines.

These options can be used to determine variable vectors, profile plots and streamlines. Fluent software provides integrated post-processing tools. However, there is nothing to prevent data being exported in a variety of formats for processing in other software packages, such as TECPLOT for visualization, or Origin for more advanced analysis.

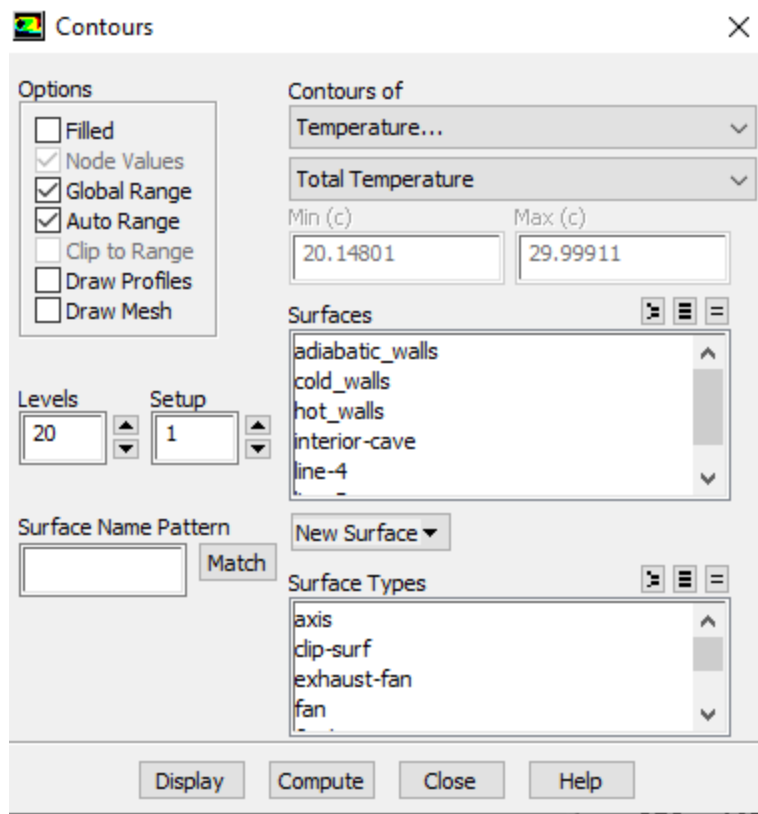


Figure III-21: calculation of temperature and displaying the isotherm line

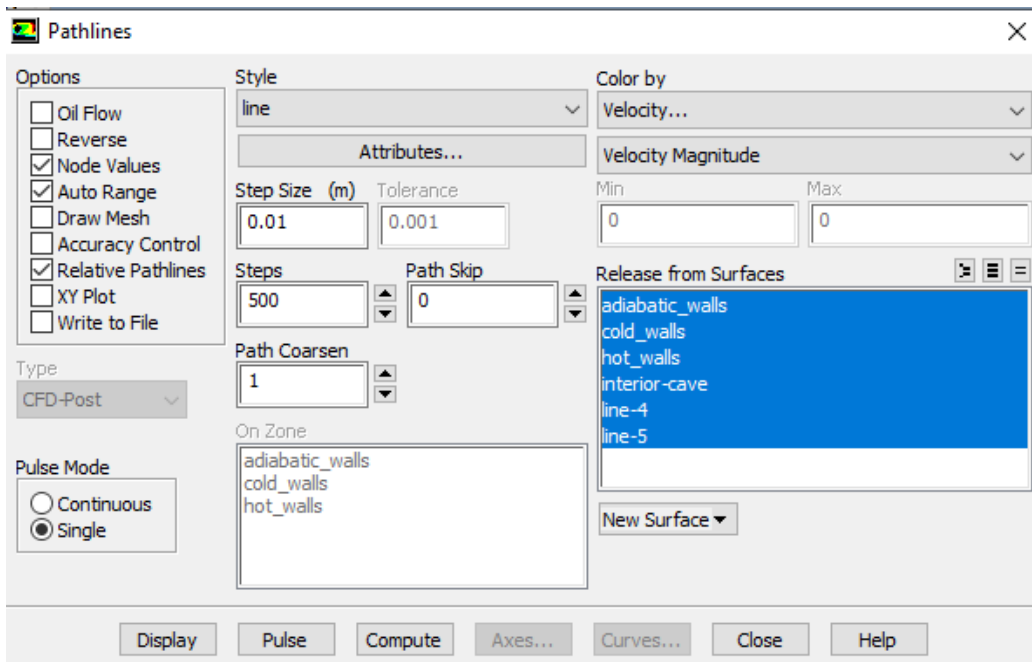


Figure III-22: displaying the pathlines.

j) Saving files:

File→ Write→ Case & Data

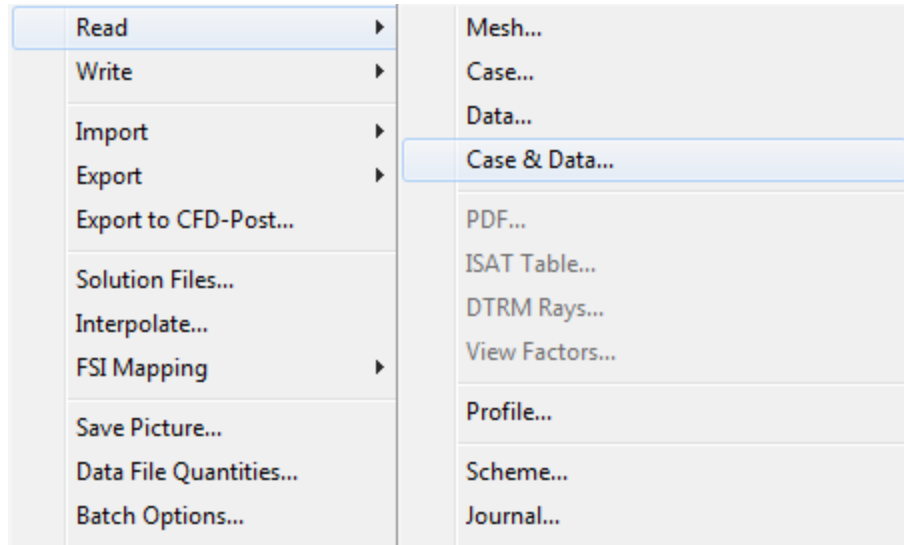


Figure III.23: Saving files.

Conclusion:

In this chapter, we have presented a detailed explanation of Ansys and how to use it, the calculation steps by the software using CFD numerical simulation.

We have included in our results the thermal and velocity fields, the streamlines and the Nusselt number, which will be displayed, explained and discussed in the next chapter.

Chapter IV

Results

& discussion

IV-1 Introduction:

In this chapter, we present the simulation results obtained using the CFD code (Ansys Fluent). Firstly, we present the independence of the mesh on the numerical calculation results as well as the comparison between the numerical results obtained and those calculated by M.Mahmoodi and S. Hashemi [28] to validate our simulation code. Next, we will study the influence of several parameters on the flow and heat transfer of (water-cu and water-TiO₂) nanofluids in the C-shaped configuration studied, such as:

- * The influence of Rayleigh number ($Ra = 10^3, 10^4, 10^5, 10^6$).
- * The influence of nanofluid solid volume fractions ($\varphi = 0, 0.03, 0.06, 0.1$).
- * The influence of different aspect ratio ($AR=0.2, 0.4, 0.6, 0.8$)

The objective is to study the influence of the Rayleigh number and the volume fraction of nanofluid on heat transfer in natural convection. In order to do this, the numerical simulation results obtained are presented in the form of:

- * Contours of streamlines;
- * Contours of isothermal lines (temperature).
- * Average Nusselt number.

IV-2 Mesh effect:

The study of the independence of the mesh on the calculation results was carried out for a configuration frequently used in the literature; this is a c-shaped enclosure filled with nanofluid (cu-water). Different mesh sizes of $21^2, 41^2, 61^2, 81^2, 91^2, 101^2, 111^2, 121^2$ were used. Figure IV-1 shows the variation of the average Nusselt number at the hot walls of the enclosure as a function of mesh refinement

for $\varphi=0.1$, $Ra = 10^6$ with different aspect ratio (AR=0.2,0.4,0.6,0.8). From this figure, it is clear that the variation of the average Nusselt number becomes stable from the mesh size of 91^2 elements. The increase in the number of nodes has no effect. Consequently, this mesh size (91×91 , Figure VI-2) will be used in all calculations. Therefore, this mesh size was selected to perform the numerical calculation for the C-shape configuration studied.

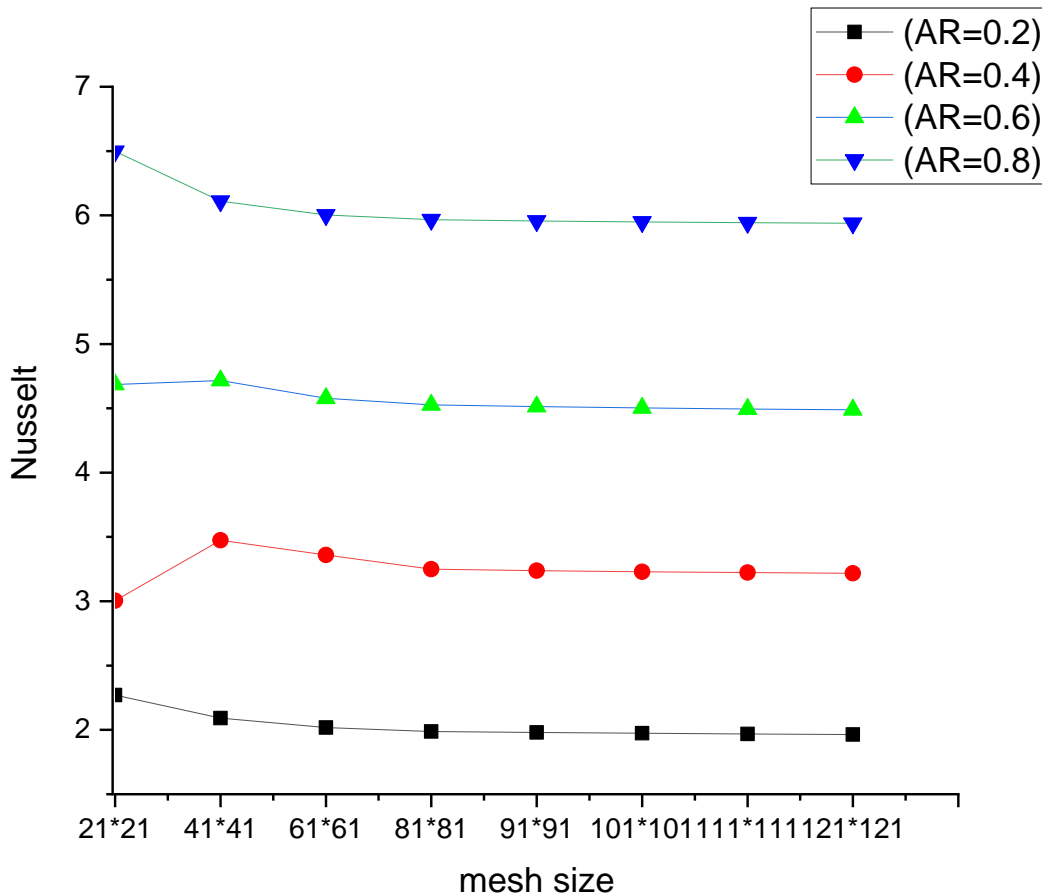


Figure IV- 1: Mesh size independence on results, for (AR=0.2,0.4,0.6,0.8), $\varphi=0.1$, $Ra = 10^6$ for water-cu.

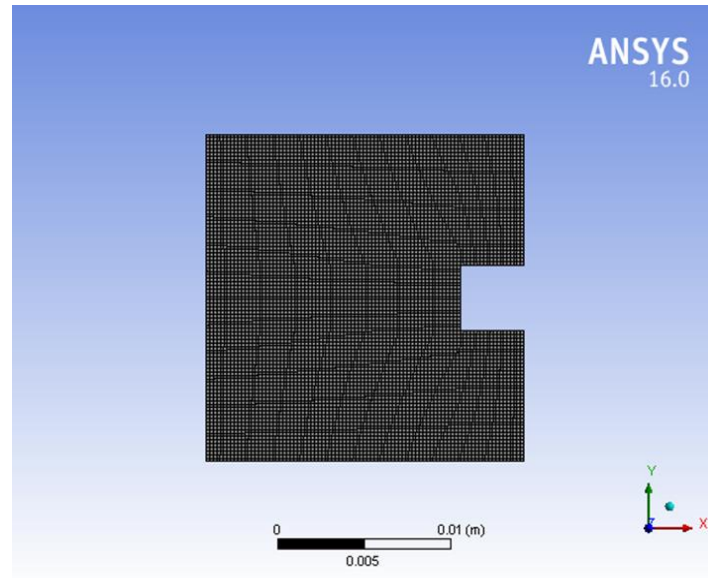
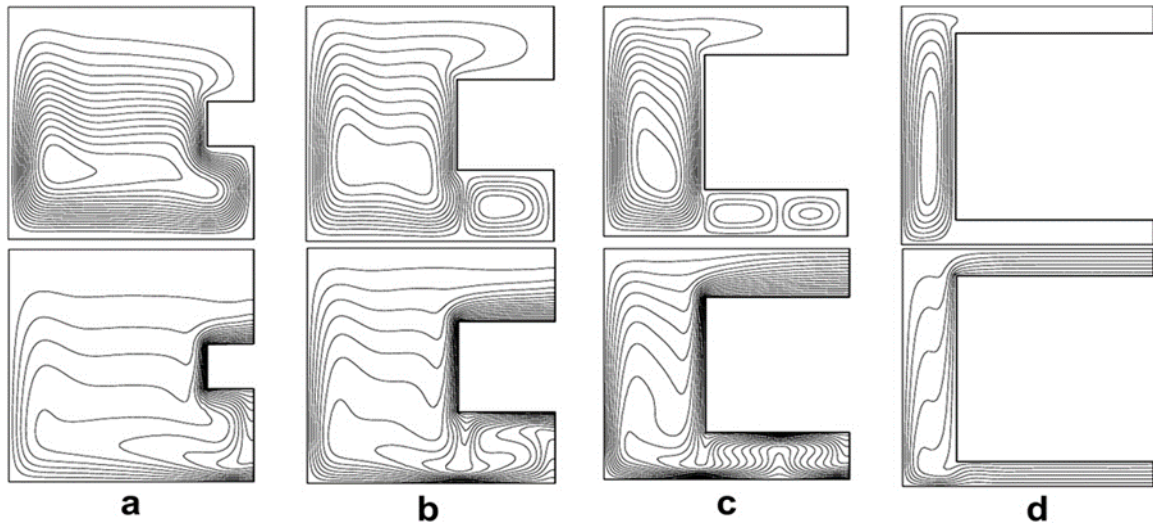


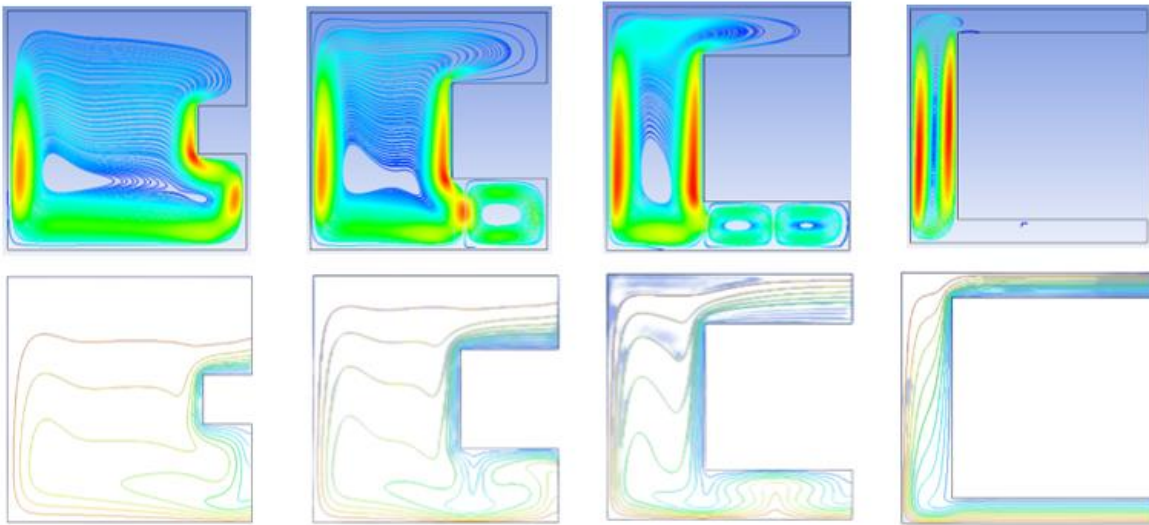
Figure IV- 2: The chosen mesh.

IV-3 Results validation:

In order to verify the accuracy of the numerical results obtained in the present work with the FLUENT code, a validation of our numerical simulation was carried out by comparing it with the numerical and experimental studies of M.Mahmoodi and S.Hashemi [28] which are available in the literature. The same conditions as in [28] were used: the convection fluid is nanofluid (water-cu) in a c-shaped geometry, we also used the same Rayleigh numbers and volume fraction (Ra, φ) as in [28].



I



II

Figure IV- 3: I- Mahmodi et Seyed [28] Streamlines (up) and isotherms (down) inside the C-shaped enclosure filled with pure fluid ($\phi=0$) at $Ra=10^6$, (a) $AR=0.2$, (b) $AR=0.4$, (c) $AR=0.6$, (d) $AR=0.8$ [28]. II present study.

In order to validate the calculation code, we compared the variation of Rayleigh number (Ra) as a function of average Nusselt number (Nu) for the pure fluid case ($\phi=0$). Figure IV-5 left shows the variation of Ra as a function of Nu found

by Mostafa Mahmoodi and Seyed Mohammad Hashemi [28], who applied the finite volume method to solve the same problem. Figure IV-5 right shows the results simulated by Ansys Fluent. A good match was found, which may give more confidence in our calculation.

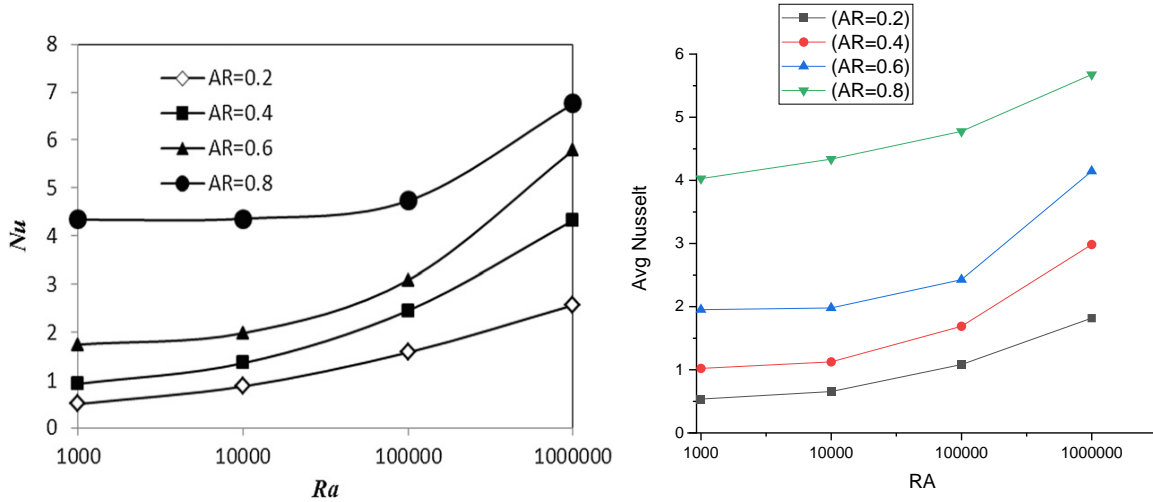


Figure IV- 5: Comparison of Rayleigh number variation as a function of mean Nusselt number for ($\phi=0$); left figure: reference results (Mostafa Mahmoodi and Seyed Mohammad Hashemi [28]); right figure: our result.

IV-4 Presentation of result:

4.1 Rayleigh number effect:

in order to examine the influence of Rayleigh number on the dynamic and thermal fields of the natural convection phenomenon in the studied C-shaped cavity for the two nanofluid studied (water-cu, water-TiO₂), the temperature contours (isotherms) and streamlines were shown for the fluid case ($\phi=0,0.1$, AR=0.2), for different Rayleigh numbers varied between 10^3 to 10^6 . Our main objective is to determine the effect of Rayleigh number on the dynamic and thermal behavior of natural convection flow.

c) For water-cu:

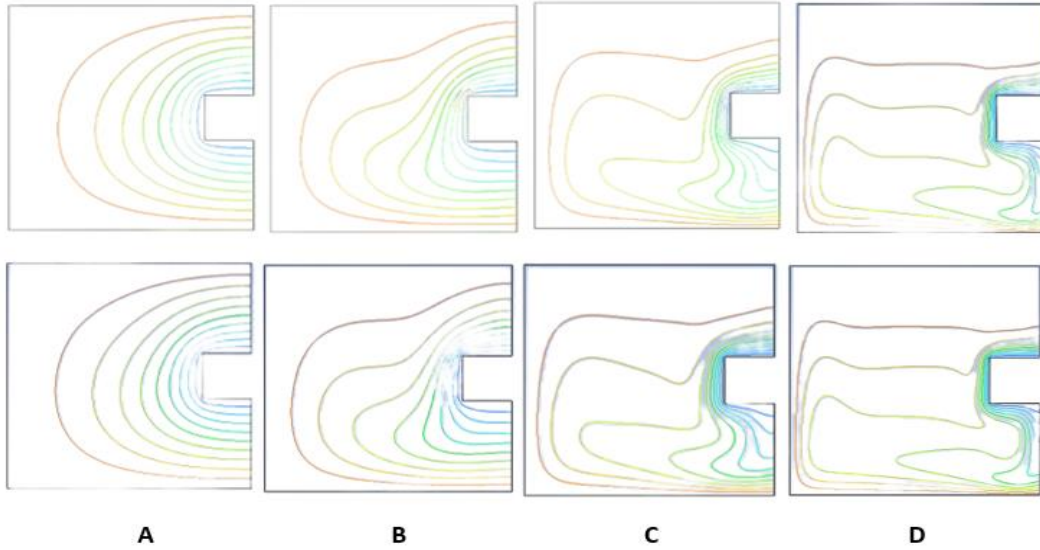


Figure IV- 6: Isotherms inside the cavity with AR=0.2 for pure fluid (up) and nanofluid water-cu with $\phi=0.1$ (down), (A) $Ra=10^3$, (B) $Ra=10^4$, (C) $Ra=10^5$, (D) $Ra=10^6$

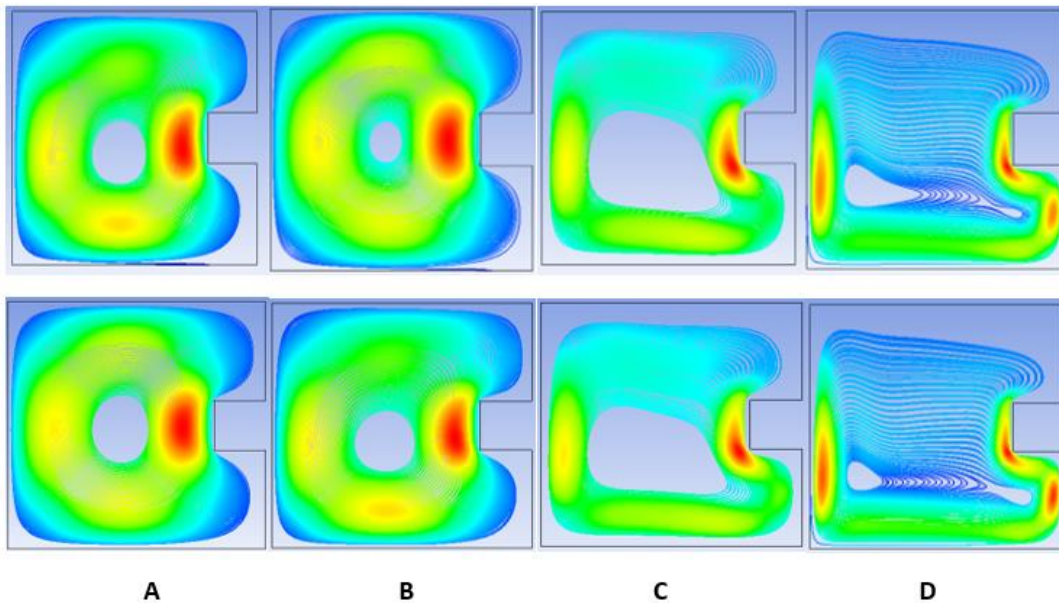


Figure IV- 7: Streamlines inside the cavity with AR=0.2 for pure fluid (up) and nanofluid water-cu with $\phi=0.1$ (down), (A) $Ra=10^3$, (B) $Ra=10^4$, (C) $Ra=10^5$, (D) $Ra=10^6$

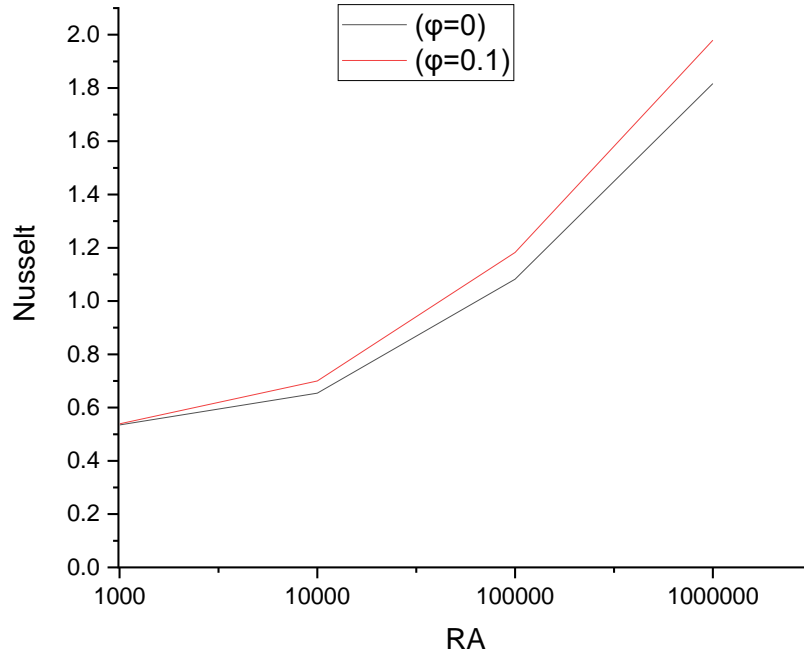


Figure IV- 8: Rayleigh number variation as a function of average Nusselt number for AR=0.2 Water-cu.

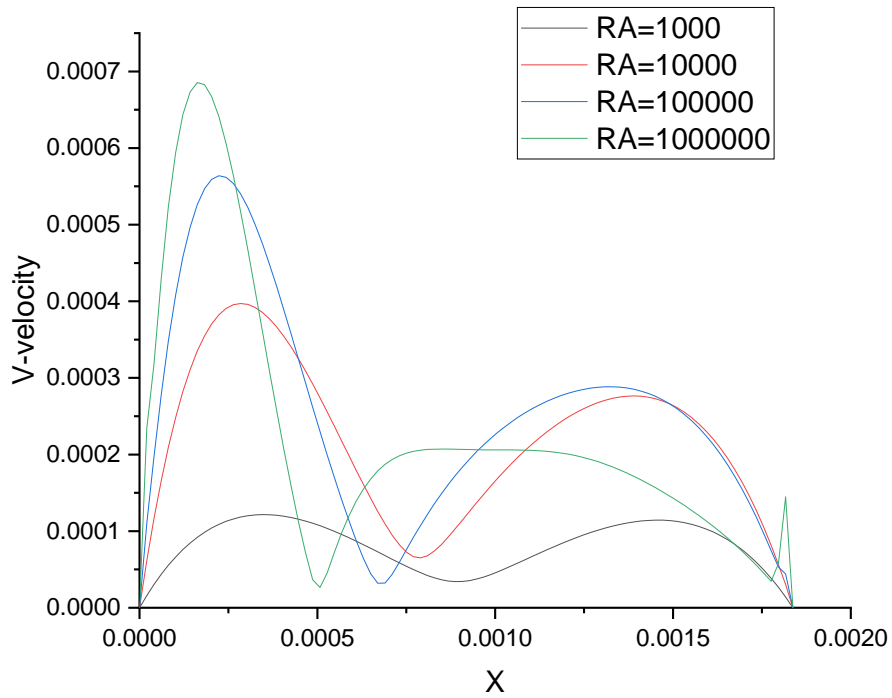


Figure IV- 9 V-velocity with AR=0.2, ($\phi=0.1$) water-cu.

Figure IV- 6 and Figure IV- 7 show the streamlines and the isotherms in the C-shaped cavity with the aspect ratio of 0.2 at different Rayleigh numbers. Moreover, as the Rayleigh number increases, the core of the eddy moves downward resulting in more densely packed streamlines at the bottom of the enclosure as compared to its top.

The shapes of the core of the eddy for the cavity filled with pure fluid and nanofluid are different.

As far as the isotherms in Figure IV- 6 are concerned, at $Ra=10^3$, they are evenly symmetrically distributed inside the enclosure demonstrating a conduction-dominated heat transfer regime.

For high Rayleigh numbers, natural convection-dominated regime, distinct thermal boundary layers are formed near to the bottom and left walls. The enclosure becomes thermally stratified. Moreover, the heat transfer in the top of the enclosure is suppressed due to diminishing the conduction effect. At high Rayleigh numbers, when the volume fraction of the nanoparticles increases, thermal boundary layers thicken and the natural convection weakens due to an increase in the viscosity of nanofluid.

Figure IV- 9 We notice that the speed is high under the vortex and relatively weak at the top of the vortex, and we also notice that the lowest value of speed is in the center of the vortex.

Regarding the effect of the Rayleigh number on the velocity it will be as follows:

$RA=10^3$ has no effect where we see that the velocity curve is symmetrical to the center of the vortex where the highest value is 0.000125 m/s and is above and below the vortex and the lowest value is 0.000025 m/s and this is in the center of the vortex.

CHAPTER IV: Results and discussion

$RA=10^4$ We observe a noticeable change where the highest value under the vortex is 0.0004 m/s, the highest value above the vortex is 0.00028 m/s and the lowest value in the center of the vortex is 0.00008 m/s.

$RA=10^5$ We note that the curve aligned in the direction of the bottom of the vortex and reached the highest value of 0.00057 m / s and that under the vortex and the highest value of the highest vortex was 0.0003 m / s and the lowest value was in the middle of the vortex 0.00005 m / s

$RA=10^6$ Here we notice the greatest difference, where the lowest velocity of a vortex was 0.00068 m/s, the highest value of the highest vortex was 0.0002 m/s, and the lowest value in the middle of the vortex at an estimated velocity of 0.00035 m/s

And from it we conclude that as the Rayleigh number increases, the effect on velocity increases significantly.

d) for Water-TiO₂:

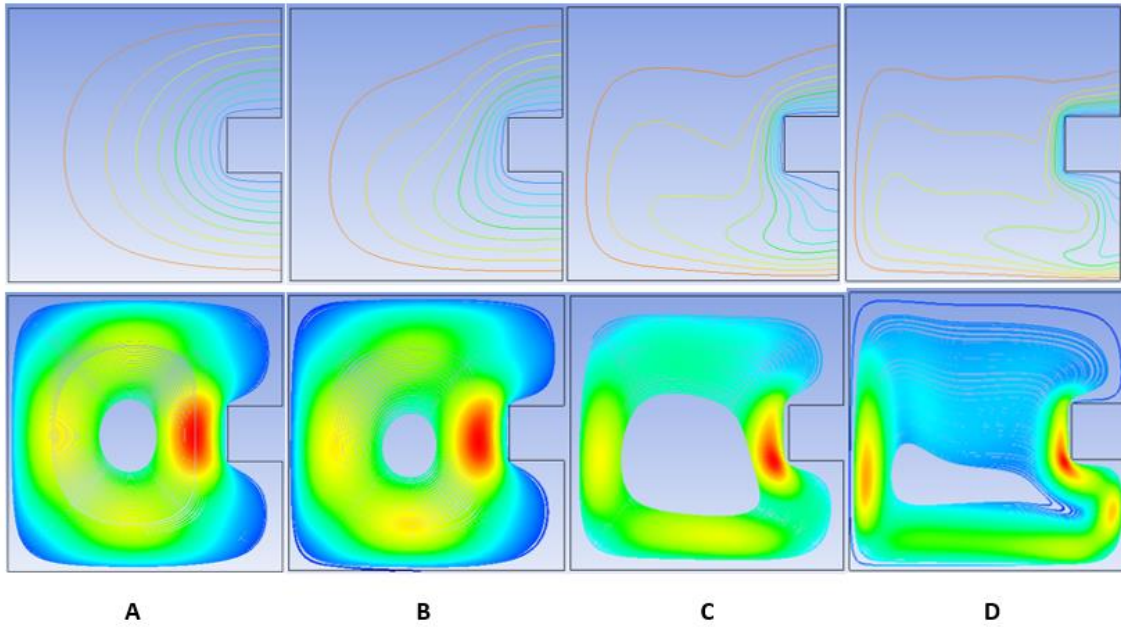


Figure IV- 10: Streamlines (down) and isotherms (up) inside the C-shaped enclosure filled with nanofluid Water-TiO₂($\phi=0.1$) at AR=0.2, (A) Ra=10³, (B) Ra=10⁴, (C) Ra=10⁵, (D) Ra=10⁶

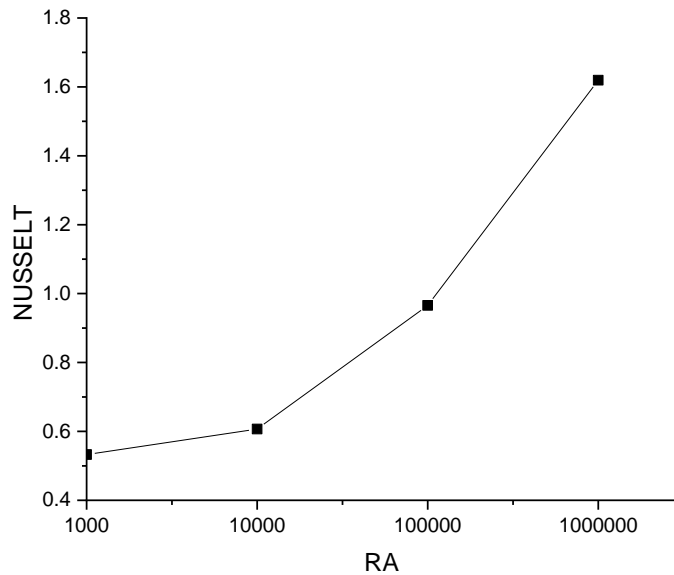


Figure IV- 11: Rayleigh number variation as a function of average Nusselt number for AR=0.2 water-TiO₂

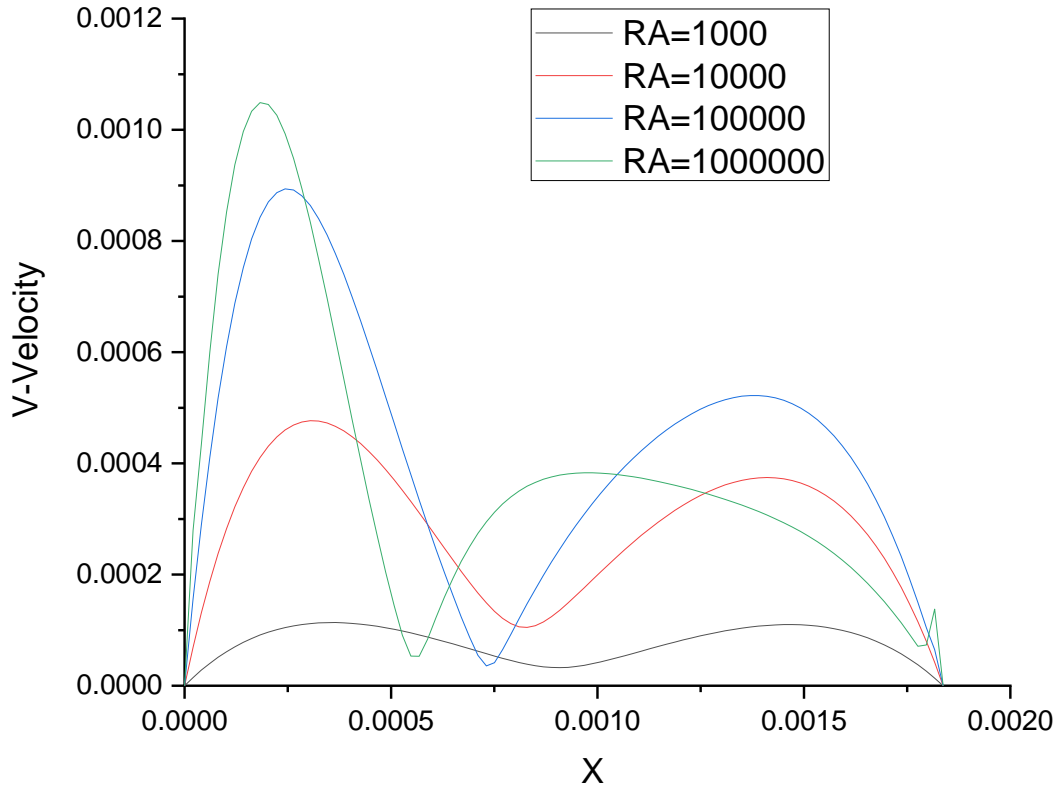


Figure IV- 12 V-velocity with AR=0.2, ($\phi=0.1$) water-TiO₂.

Figure IV- 12 RA=10³ we note the same effect as the water-cu the difference is in the velocity where is the highest value is 0.0001 m/s and is above and below the vortex and the lowest value is 0.000021 m/s and this is in the center of the vortex

RA=10⁴ We observe a noticeable change where the highest value under the vortex is 0.0005 m/s, the highest value above the vortex is 0.0004 m/s and the lowest value in the center of the vortex is 0.0001 m/s.

RA=10⁵ We note that the curve aligned in the direction of the bottom of the vortex and reached the highest value of 0.0009 m / s and that under the vortex and the highest value of the highest vortex was 0.00055 m / s and the lowest value was in the middle of the vortex 0.000048 m / s

RA=10⁶ Here we notice the greatest difference, where the lowest velocity of a vortex was 0.0018 m/s, the highest value of the highest vortex was 0.0004 m/s, and the lowest value in the middle of the vortex at an estimated velocity of 0.00005 m/s

And from it we can we reach the same conclusion as the water-cu that as the Rayleigh number increases, the effect on velocity increases significantly.

4.2 effect of aspect ratio:

to check the influence of the aspect ratio, we will present the temperature contours (isotherms) and streamlines for the fluid case ($\varphi=0.1$, RA=10⁶), for different AR varied between 0.2 to 0.8. Our main objective is to determine the effect of aspect ratio change on the dynamic and thermal behavior of natural convection flow.

a) for water-cu:

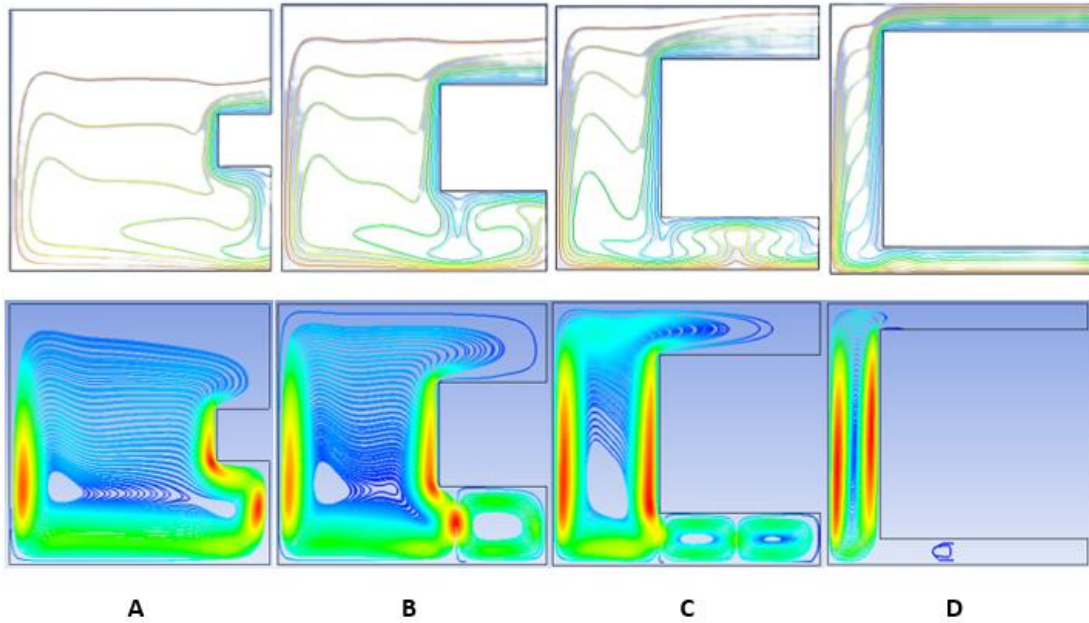


Figure IV- 13: Streamlines (down) and isotherms (up) inside the C-shaped enclosure filled with nanofluid water-cu ($\phi=0.1$) at $Ra=10^6$, (A) $AR=0.2$, (B) $AR=0.4$, (C) $AR=0.6$, (D) $AR=0.8$.

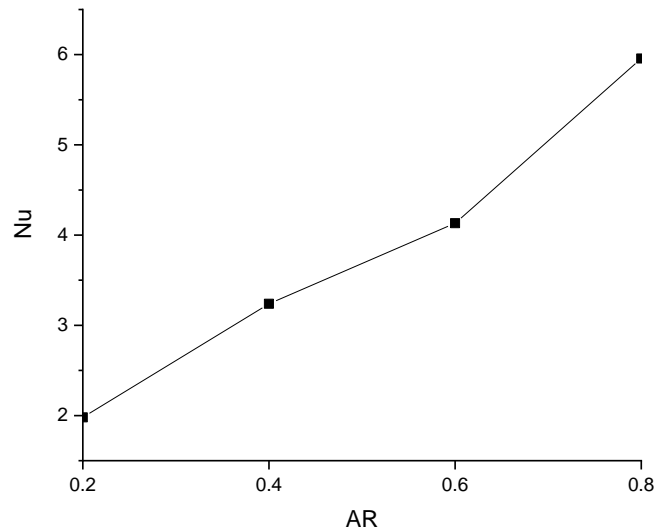


Figure IV- 14: average Nusselt number variation as a function of aspect ratio for ($\phi=0.1$, $RA=10^6$) water-cu.

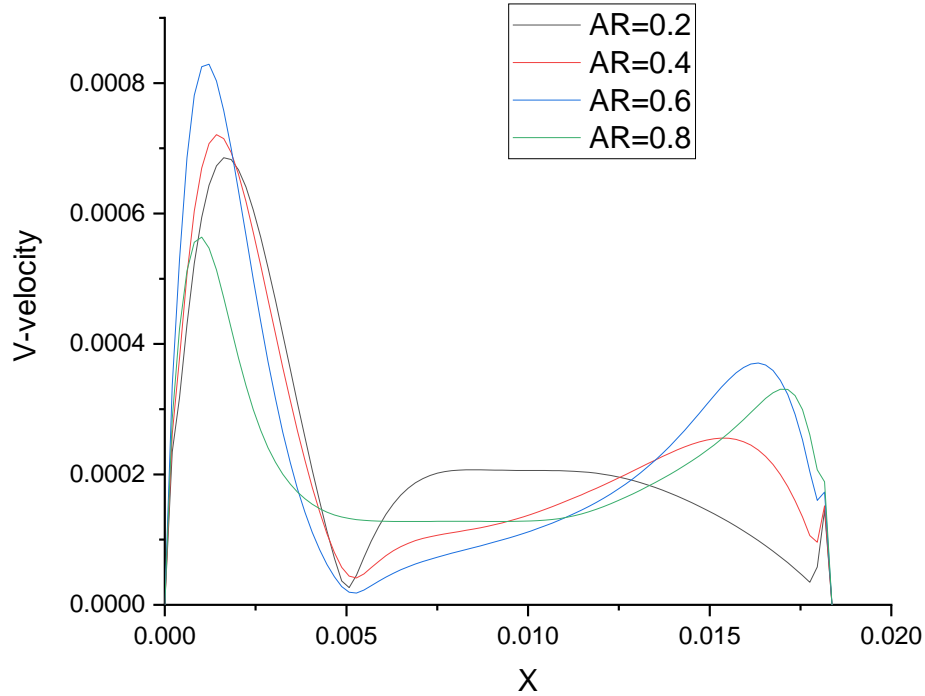


Figure IV- 15 V-velocity with $RA=10^6$, ($\phi=0.1$) water-cu.

Figure IV- 13 illustrates effect of increase in AR on flow pattern and temperature distribution inside the enclosures filled with nanofluid ($\phi=0.1$) at $Ra=10^6$.

For $AR=0.2$, the nanofluid is heated by the hot wall and expands as it moves upwards. The nanofluid is cooled by cold wall and compressed as it moves downwards. Therefore, a clockwise vortex is generated in the entire enclosure. This aspect ratio isotherm is condensed near the top of the cold wall. This means that the top cold wall has small effect on nanofluid cooling.

For $AR = 0.4$, the eddy splits into two counter-rotating eddies. The large vortex rotates clockwise and is on the left side of the enclosure, and the smaller counterclockwise vortex is below the cold wall.

For $AR = 0.6$, two eddies form under the cold wall. The right and left eddies are clockwise and counterclockwise respectively.

For $AR=0.8$, multicellular flow patterns do not occur under the cold wall. This is because there is a small gap between the hot bottom wall and the cold wall, restricting flow movement. Furthermore, as the C-shaped enclosure narrows, the local Rayleigh number and buoyancy in the region between the cold wall and bottom wall decrease. Benard cells are therefore not shaped. The corresponding isotherm shows that thermal stratification occurs in the gap above and below the cold wall for $AR=0.8$. Also note that the isotherm becomes more uniformly distributed at the top of the cold wall as the aspect ratio of the cavity increases. Observations determine the maximal and minimal limits of Rayleigh Benard cell development in the gap between the hot bottom wall and the cold rib.

b) for Water-TiO₂:

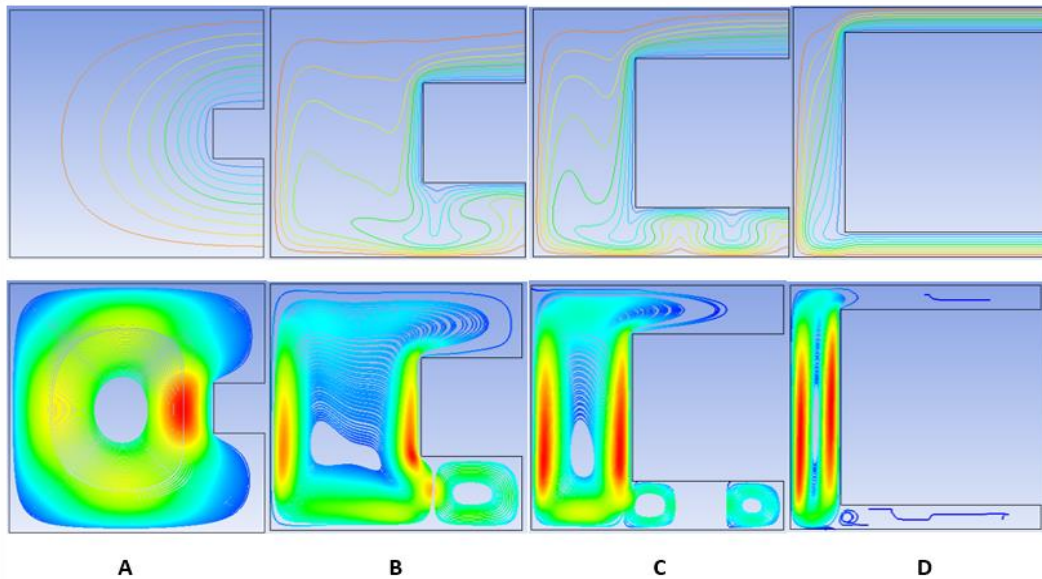


Figure IV- 16: Streamlines (down) and isotherms (up) inside the C-shaped enclosure filled with nanofluid water-TiO₂ ($\phi=0.1$) at $Ra=10^6$, (A) $AR=0.2$, (B) $AR=0.4$, (C) $AR=0.6$, (D) $AR=0.8$.

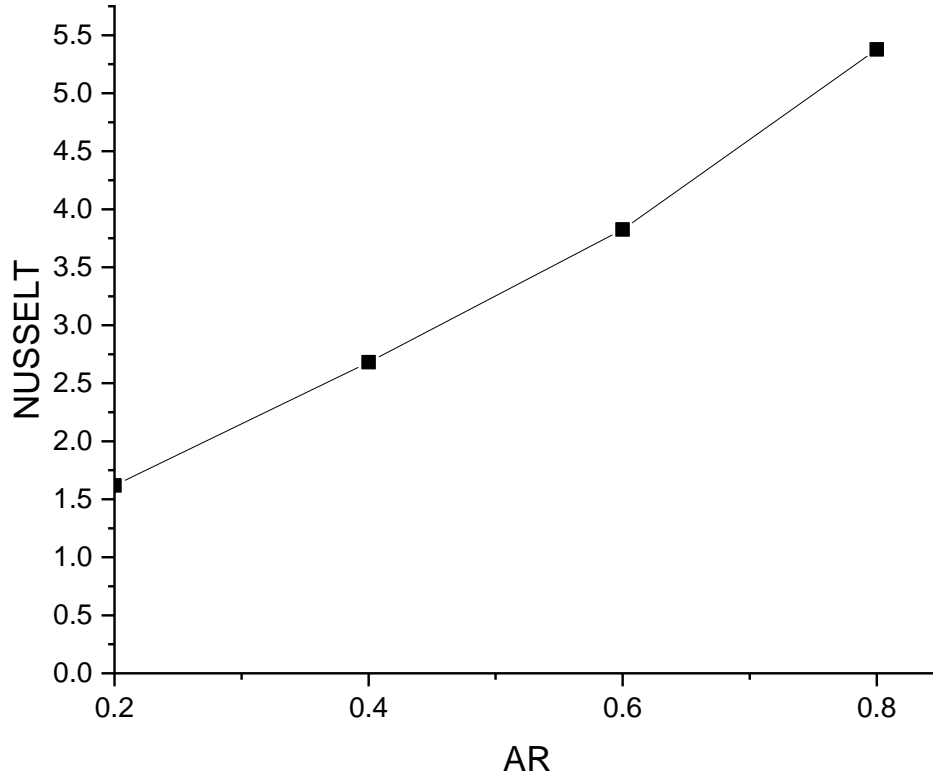


Figure IV- 17: average Nusselt number as a function of aspect ratio number for ($\phi=0.1$, $RA=10^6$) water-TiO₂.

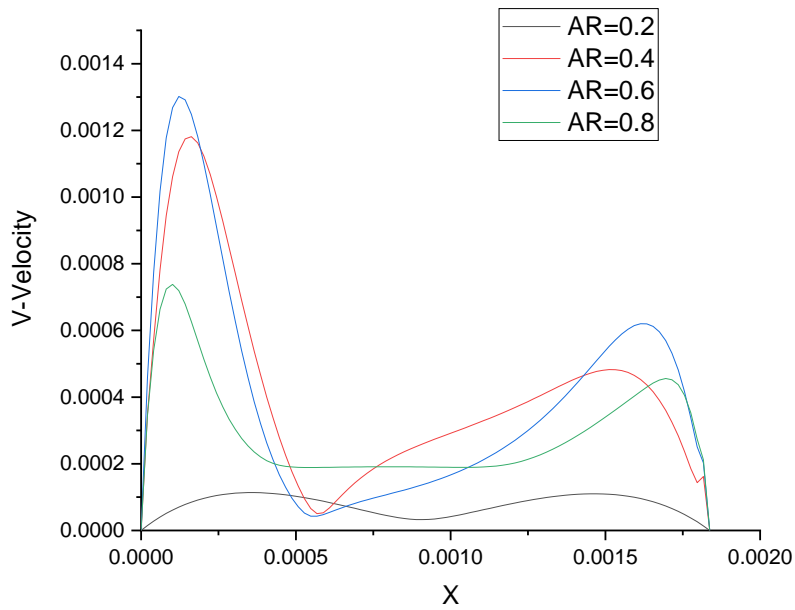


Figure IV- 18 V-velocity with $RA=10^6$, ($\phi=0.1$) water-TiO₂.

4.3 volume fraction effect:

For Water-cu:

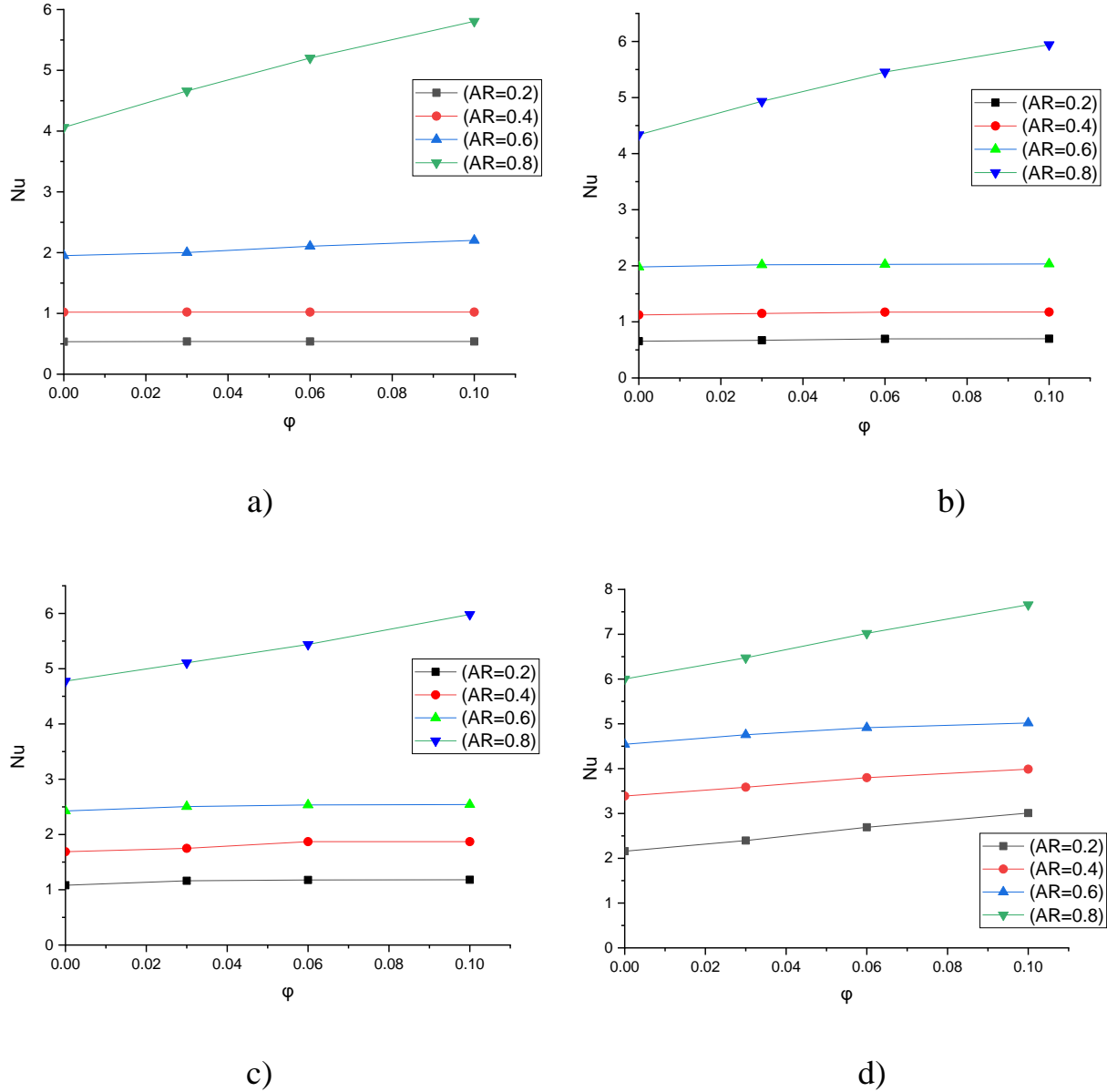


Figure IV- 19: Variation of average Nusselt number with nanoparticles volume fraction for different aspect ratios of enclosure filled with nanofluid water-cu, (a) $Ra=10^3$, (b) $Ra=10^4$, (c) $Ra=10^5$, (d) $Ra=10^6$.

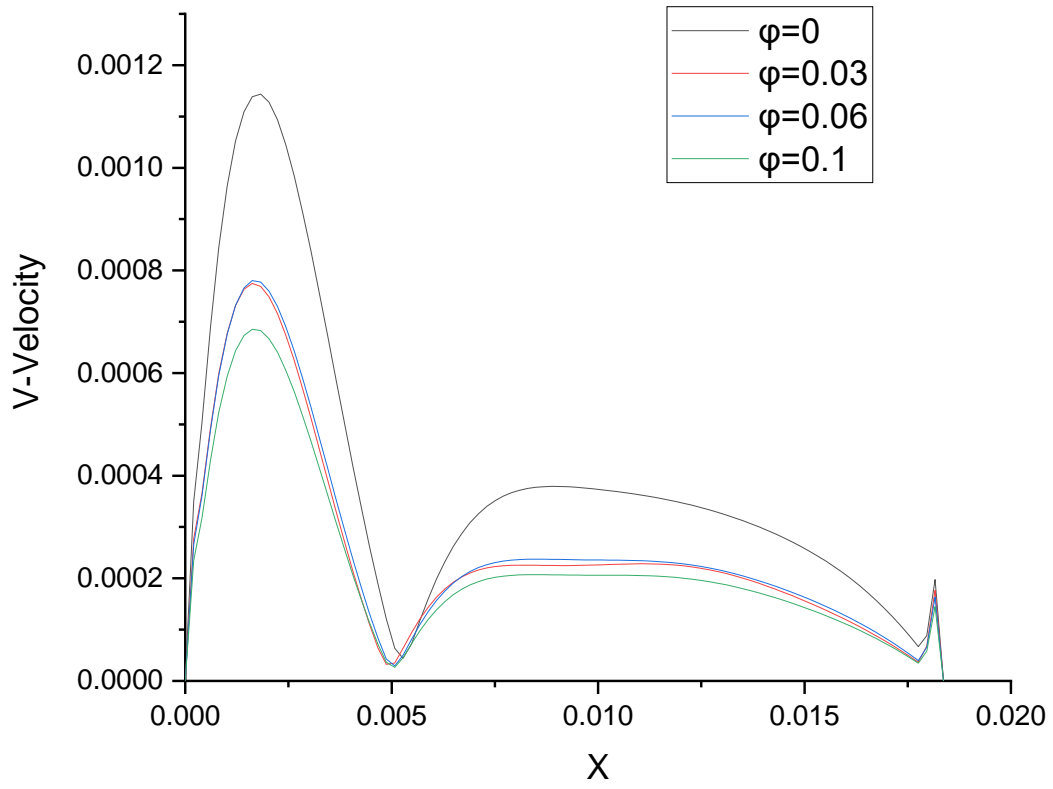


Figure IV- 20 V-velocity with $RA=10^6$, $AR=0.2$ for water-cu.

For water- TiO₂:

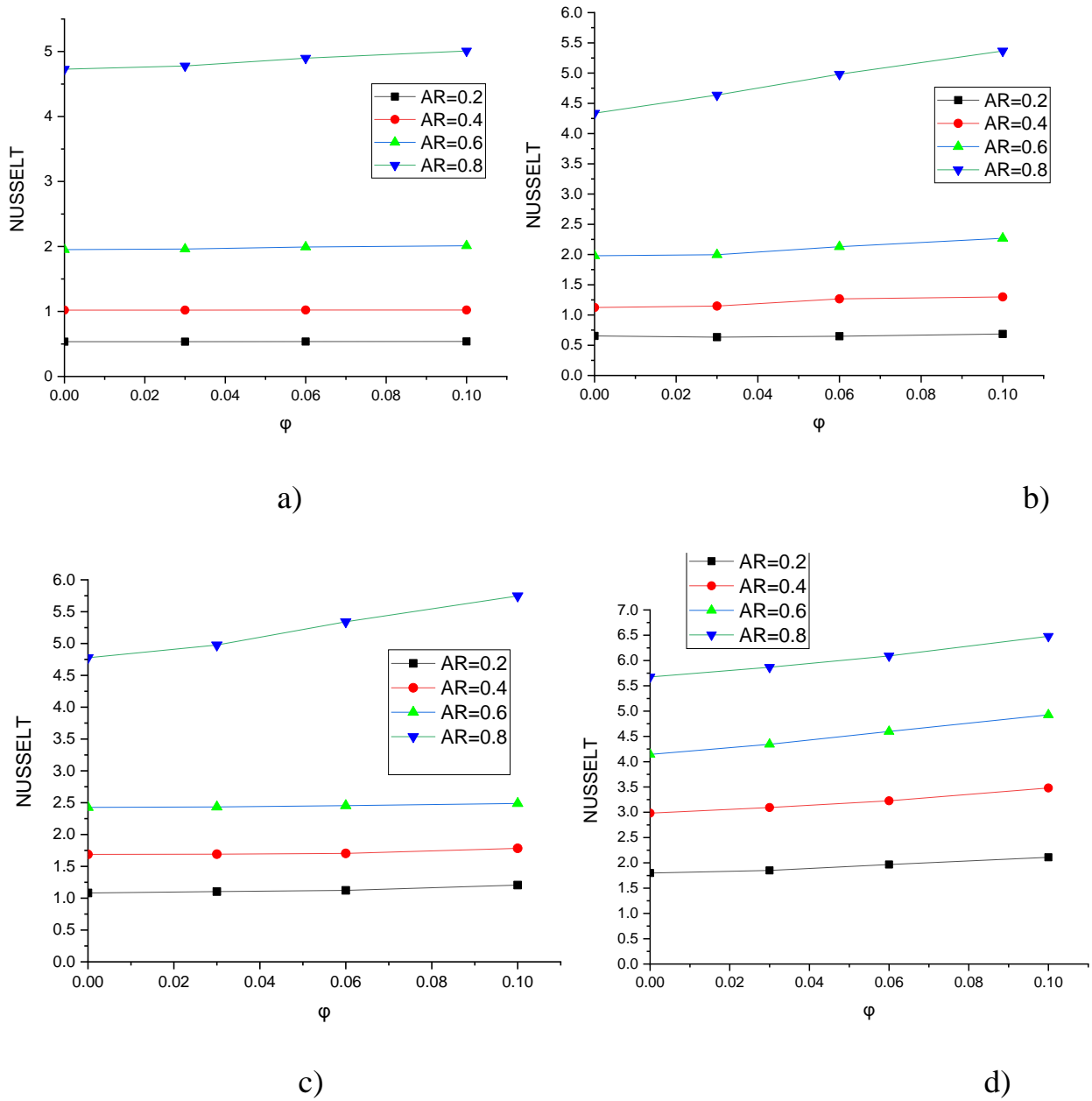


Figure IV- 21: Variation of average Nusselt number with nanoparticles volume fraction for different aspect ratios of enclosure filled with nanofluid water- TiO₂, (a) Ra=10³, (b) Ra=10⁴, (c) Ra=10⁵, (d) Ra=10⁶.

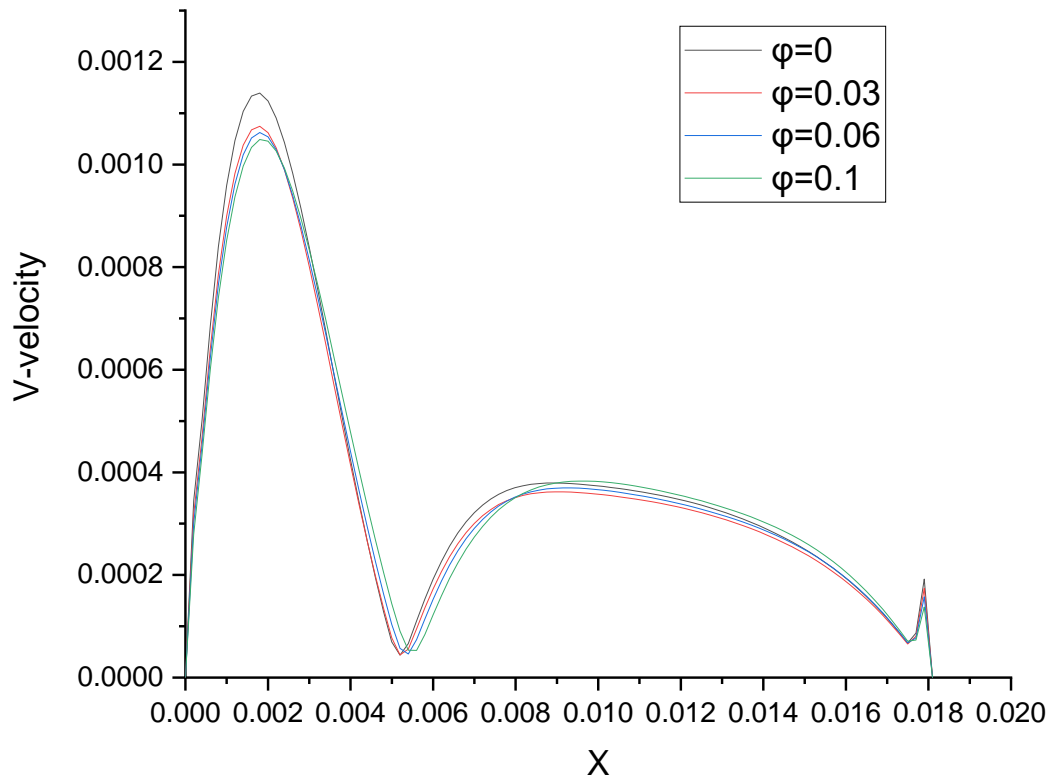


Figure IV- 22 V-velocity with $RA=10^6$, $AR=0.2$ for water- TiO_2

GENERAL CONCLUSION:

This study focuses on the simulation of natural laminar convection in a C-shaped cavity filled with nanofluid (water-cu). The main objective is to see the impact of the volume fraction of the nanoparticles on the heat transfer rate.

The problem was approached using a numerical approach based on the finite volume method using a CFD code (Ansys Fluent) (version 2016).

The influence of the Rayleigh number as well as the influence of the volume fraction of nanofluid ($\phi=0\sim 0.1$) on the thermal and dynamic structures of the flow and on heat transfer was investigated numerically, by determining the contours of the streamlines and isotherms, as well as the variations in the Nusselt number.

The following conclusions were reached in the course of this study:

- * The nanofluid produces a higher heat transfer rate at high Rayleigh number values.
- * At moderate Rayleigh numbers, the nanofluid shows no significant improvement in heat transfer compared to the pure fluid.
- * Increasing the Rayleigh number increases the heat transfer rate for both nanofluid and pure fluid.
- * The rate of increase in the average Nusselt number is higher at higher Rayleigh numbers.
- * We conclude that water-cu has more efficient heat exchange than water-TiO₂ based on the Nusselt number.

Perspectives:

As perspectives related to this work, we propose:

- Numerically or experimentally study new geometric configurations to improve heat transfer by natural convection.
- studying new combination of nanofluids such as (water-Ag, water-Al₂O₃).

BIBLIOGRAPHY:

[1] - T.L. Bergman, F.P. Incropera, A.S. Lavine, D.P. DeWitt, « Introduction to heat transfer », second edition, John Wiley & Sons, (2011)

[2]- L. Benkezim, « Simulation numérique de la convection naturelle d'un nanofluid dans une cavité rectangulaire », Thèse de magistère, Université M'hamed Bougara-Boumerdes, (2013).

[3]- S. Mojumder, S. Saha, S.Saha, M.A.H. Mamun, « Effect of magnetic field on natural convection in a C-shaped cavity filled with ferrofluid », *Procedia Engineering*, Vol. 105pp. 96 – 104, (2015).

[4]- S.U.S. Choi, « Enhancing thermal conductivity of fluids with nanoparticles », *ASME Fluids Eng. Division* 231 99–105. (1995).

[5]- A. M. Hussein, K.V. Sharma, R. A. Bakar, K. Kadirgama, « A review of forced convection heat transfer enhancement and hydrodynamic characteristics of a nanofluid, *Renew ». Sust. Energy Rev. Vol. 29, pp. 734-743,*

[6]- H. Lanez, « Optimisation du bilan thermique d'un circuit de refroidissement du solvant Lourd en présence du phénomène d'encrassement », mémoire de master, université Echahid Hamma.

[7]- M.Bordjane, «cours modes transfert thermique», 3ème année licence, Université Mohamed Boudiaf, Oran- Algérie (2017).

[8]- Y. Jannot, P. Meukarm. Simplified estimation method for determination of thermal effusivity and thermal conductivity with a low cost hot strip, *measurement science and Technology*, vol.15, pp.1932-1938, (2004).

BIBLIOGRAPHY

- [9]-J.L.Battaglia, A.Kusiak et J.R.Puiggali, «Introduction aux transferts thermiques», cour et exercices corrigés 2^{ème} édition licence (2010).
- [10]- S. Saddam, «Amélioration de la convection mixte dans un dissipateur de chaleur à ailette elliptique creuse », mémoire de master, Université Mohamed Boudiaf M'silla- Algérie, année universitaire 2014-2015.
- [11]- M. Benmerabet, «Modélisation et simulation des phénomènes de transfert thermique par convection assistés par le mouvement fluide», mémoire de master, Université Badji Mokhtar Annaba- Algérie , année universitaire 2016-2017.
- [12]- Ali Agha Hamza.Initiation aux transfert thermiques.2019
- [13]- C. Chin-Hsiang, H. Wen-Hsiung, « Numericalprediction for laminarforced convection in parallel-plate channelswith transverse fin arrays» , International Journal of Heat and Mass Transfer, (1991).
- [14]- E K Fatima, G Kamal, M-L Samir : 'La Convection Naturelle Des Nano-fluides En Cavité Rectangulaire Verticale',Casablanca(Maroc) ,2014.
- [15]- Hamdi M, Hedia W, Ridha D, EzeddineS: 'Accurate finite volume investigation of nano-fluid mixed convection in two-sided lid driven cavity including discrete heat sources',Univ. Tunis El-Manar, Tunisia, 2015.
- [16]- Billel B, Salah L, El Hacene M : 'Etude Numérique De La Convection Naturelle Dans Une Cavité Rectangulaire Contenant Un Nano-fluide',Université 20 Août 1955 De Skikda, 2015.
- [17]- M. El Hafad Bara, Mme. SakinaE, 'Etude Numérique De La Convection Naturelle Du Mélange Eau-Cu Dans Une Cavité Partiellement Chauffée',Université De La Rochelle, Av. Michel Crépeau, 17042 La Rochelle Cedex 1, France, 2017

BIBLIOGRAPHY

- [18]- Boutra, A., et al., "Numerical study of mixed convection heat transfer in a square cavity filled with a nanofluid," *International Journal of Thermal Sciences*, vol. 49, no. 9, pp. 1663-1671, 2010.
- [19]- Soufi EH: 'Application Des nano-fluids Pour Le Refroidissement : Etude D'un Cas D'une Géométrie Simple', Université Kasdi Merbah d'Ouargla, 2013.23- S. U. S. Choi, Z. G. Zhang, W. Yu, F. E. Lockwood, and E. A. Grulke, "Anomalous thermal conductivity enhancement in nanotube suspensions," *Appl. Phys. Lett.*, vol. 79, no. 14, pp. 2252–2254, Oct. 2001, doi: 10.1063/1.1408272.
- [20]- P. Keblinski, J. A. Eastman, and D. G. Cahill, "Nanofluids for thermal transport," *Mater. Today*, vol. 8, no. 6, pp. 36–44, Jun. 2005, doi: 10.1016/S1369-7021(05)70936- 6.
- [21]- M. F. A. DAAS, S. DERFOUF, N. BELGHAR, "Simulation numérique de l'échange thermique dans une enceinte rectangulaire," *Third Int. Conf. Energy, Mater. Appl. Energ. Pollution.*, no. ICEMAE p 2016.
- [22]- Z. B. et R. S. k. Najid, F. Dahami, "Modélisation de l'échange thermique par convection naturelle de nano fluide (Cu-eau) dans une enceinte à paroi ondulée," 13ème Congrès de Mécanique.
- [23]- S. TABET, "Etude numérique de la convection naturelle dans une enceinte fermée partiellement chauffée," Université d'Oran 2, 2017.
- [24]- KROUMA Saadia, "Influence de la géométrie des nanoparticules dans un nano fluide sur le transfert thermique," Université de Khider Mohamed Biskra, 2017
- [25]- M. El-Hattab et al., « Simulation numérique de la convection naturelle des nanofluides dans une enceinte carrée chauffée par une source de chaleur », *Revue*

BIBLIOGRAPHY

internationale d'héliotechnique, Ecole National des Sciences appliquées, B.P. 1136, Agadir, Maroc, (2013)

[26]- S.M. Aminossadati., « Hydromagnetic natural cooling of a triangular heat source in a triangular cavity with water–CuO nanofluid », International Communications in Heat and Mass Transfer, vol. 43, pp. 22–29, (2013).

[27]-A. Bouhelal, S. Lebbihi, N. Benrachi, A. Smaili, « Simulation de la convection naturelle autour d'une source de chaleur localisée au fond d'une enceinte remplie de nanofluide », CFD & Tech conférence, CRND-Draria, Alger, 02 – 03 Mai, (2016).

[28]- Mahmoodi, M., & Hashemi, S. M. (2012). Numerical simulation of free convection in a C-shaped enclosure filled with Cu-water nanofluid. International Journal of Thermal Sciences, 55, 76-89. doi: 10.1016/j.ijthermalsci.2012.05.007.

[29]- <https://stock.adobe.com/search>